POLITECNICO DI TORINO
Repository ISTITUZIONALE

Reverse Engineering of TopHat: Splice Junction Mapper for Improving Computational Aspect

Original
Reverse Engineering of TopHat: Splice Junction Mapper for Improving Computational Aspect / Terzo, Olivier; Mossucca, L; Acquaviva, Andrea; Abate, Francesco; Ficarra, Elisa; Provenzano, R.. - ELETTRONICO. - (2012). (ISMS 2012 - 3rd International Conference on Intelligent Systems, Modelling and Simulation Kota Kinabalu 8 – 10 February 2012) [10.1109/ISMS.2012.76].

Availability:
This version is available at: 11583/2497850 since:

Publisher:

Published
DOI:10.1109/ISMS.2012.76

Terms of use:

This article is made available under terms and conditions as specified in the corresponding bibliographic description in the repository

Publisher copyright

(Article begins on next page)

08 May 2026

Nonlinearity

LONDON MATHEMATICAL SOCIETY EST. 1865

IOP Publishing

PAPER • **OPEN ACCESS**

A Hamilton–Jacobi approach to nonlocal kinetic equations

To cite this article: Nadia Loy and Benoît Perthame 2024 *Nonlinearity* **37** 105019

View the article online for updates and enhancements.

You may also like

- Self-similar solutions of the one-dimensional Landau–Lifshitz–Gilbert equation
Susana Gutiérrez and André de Laire
- Internal ring waves in a three-layer fluid on a current with a constant vertical shear
D Tseluiko, N S Alharthi, R Barros et al.
- The Ostrovsky–Vakhnenko equation by a Riemann–Hilbert approach
Anne Boutet de Monvel and Dmitry Shepelsky

This content was downloaded from IP address 130.192.232.226 on 16/09/2024 at 11:33

OPEN ACCESS
IOP Publishing | London Mathematical Society Nonlinearity
Nonlinearity **37** (2024) 105019 (35pp) https://doi.org/10.1088/1361-6544/ad75dd

A Hamilton–Jacobi approach to nonlocal kinetic equations

Nadia Loy[1,*] **and Benoît Perthame**[2]

[1] Department of Mathematical Sciences 'G. L. Lagrange', Politecnico di Torino, Corso Duca degli Abruzzi 24, 10129 Torino, Italy
[2] Sorbonne Université, CNRS, Université de Paris, Inria, Laboratoire Jacques-Louis Lions, F-75005 Paris, France

E-mail: nadia.loy@polito.it and benoit.perthame@sorbonne-universite.fr

Received 28 January 2024; revised 18 July 2024
Accepted for publication 30 August 2024
Published 13 September 2024

Recommended by Dr Claude Le Bris

Abstract

Highly concentrated patterns have been observed in a spatially heterogeneous, nonlocal, kinetic model with BGK type operators implementing a velocity-jump process for cell migration, directed by the nonlocal sensing of either an external signal or the cell population density itself. We describe, in an asymptotic regime, the precise profile of these concentrations which, at the macroscale, are Dirac masses. Because Dirac concentrations look like Gaussian potentials, we use the Hopf–Cole transform to calculate the potential adapted to the problem. This potential, as in other similar situations, is obtained through the viscosity solutions of a Hamilton–Jacobi equation. We begin with the linear case, when the heterogeneous external signal is given, and we show that the concentration profile obtained after the diffusion approximation is not correct and is a simple eikonal approximation of the true H–J equation. Its heterogeneous nature leads us to develop a new analysis of the implicit equation defining the Hamiltonian and a new condition to circumvent the 'dimensionality problem'. In the nonlinear case, when the signal occurs from the cell density itself, it is shown that the already observed linear instability (pattern formation)

* Author to whom any correspondence should be addressed.

Original Content from this work may be used under the terms of the Creative Commons Attribution 3.0 licence. Any further distribution of this work must maintain attribution to the author(s) and the title of the work, journal citation and DOI.

© 2024 The Author(s). Published by IOP Publishing Ltd and the London Mathematical Society

occurs when the Hamiltonian is convex-concave, a striking new feature of our approach.

Keywords: Hopf–Cole transform, BGK equation, Hamilton–Jacobi equation, aggregation solution, nonlocal kinetic equation

Mathematics Subject Classification numbers: 35Q20, 35Q92, 45K05

Introduction

Kinetic equations have proved to be an effective mathematical framework for modeling cell migration, both for bacteria [11, 13, 21, 22, 25, 38, 39] and for cells in a tissue [14, 24, 33–35]. In fact, the typical migration mode of a cell is the *run and tumble*, consisting in alternating runs over straight lines and reorientations, that may be biased by the presence of external signals affecting the choice of the direction, such as, for example, chemicals or the cell population density itself. At the population, or aggregate, level, the latter process may give rise to a tactic dynamics such as chemotaxis and cell-cell adhesion, respectively. Specifically, chemotaxis is the migration of cells towards an increasing gradient or concentration of a fixed chemical, while cell-cell adhesion is the tendency of cells to establish junctions in order to adhere and form tissues or cells aggregates. The run and tumble process may be modelled as a microscopic stochastic process named *velocity-jump process* [41]. It is a Markovian process that prescribes a *transition probability* T of choosing a new velocity and a *frequency of reorientation* μ. In particular, the transition probability $T = T[\mathcal{S}]$ may be influenced by the presence of an external signal $\mathcal{S}$, that may embody the presence of a chemoattractant or of the cell population density. The kinetic equation that implements a velocity-jump process of intensity $\mu > 0$, that is a piecewise deterministic Markov process in which we consider a transition probability $T[\mathcal{S}]$, may be written as

$$\partial_t f(t,x,v,\hat{v}) + \mathbf{v}\cdot\nabla_x f(t,x,v,\hat{v}) = \mu\left(\rho(t,x)\,T[\mathcal{S}](v,\hat{v}) - f(t,x,v,\hat{v})\right), \tag{1}$$

where $f = f(t,x,v,\hat{v})$ is a probability density function describing the distribution of the cell located at position $x \in \Omega \in \mathbb{R}^d$, moving with speed $v \in [0,U]$ along direction $\hat{v} \in \mathbb{S}^{d-1}$, for each time $t > 0$. We also use the notation $\mathbf{v}$ for the microscopic velocity of the cells that is given by the vector $\mathbf{v} = v\hat{v}$. As $(v,\hat{v}) \in \mathcal{V} := [0,U]\times\mathbb{S}^{d-1}$, then $\mathbf{v} \in B(0,U)$, that is compact in $\mathbb{R}^d$ and symmetric. The function $\rho(t,x)$ denotes the number density of cells in position x at time t:

$$\rho(t,x) = \int_{\mathcal{V}} f(t,x,v,\hat{v})\,\mathrm{d}v\mathrm{d}\hat{v}, \qquad (t,x) \in \mathbb{R}_+\times\Omega.$$

Formally, (1) is a kinetic equation with linear relaxation operator of BGK type.

Another important issue in modeling cell migration is the nonvanishing size of the cell that gives rise to nonlocality in the physical space (see e.g. [1, 15] and references therein). Specifically at the kinetic level, a nonlocal gradient of the chemoattractant $\mathcal{S}$ sensed with a sampling radius has been introduced in [26, 38]. In [16, 17, 34, 35, 37] the authors propose some models in which T depends on a fixed external signal $\mathcal{S}$ and also consider the case in which $\mathcal{S}$ is the cell density ρ, thus mimicking adhesion. In [34, 35] the authors derive the so called macroscopic models for the aggregate quantities defined as averaged quantities (the statistical moments of f), showing that keeping the nonlocality at the aggregate description implies a strong nonvanishing advection term. In such models, aggregation and concentrations have been observed in the cell density ρ, both in the case of linear models (i.e. T depends on $\mathcal{S}$),

and nonlinear ones (i.e. T depends on ρ). In particular, in [36] a linear stability analysis of a nonlocal kinetic model with adhesion (i.e. (1) with $\mathcal{S}=\rho$) is performed and pattern formation is shown.

Pattern formation may be seen in this context as a formation of small concentrations, typically persisting in time, being a concentration a maximum of the macroscopic density ρ. As a matter of fact, this kind of solution may be represented, at the macroscopic scale, as the sum of Dirac masses

$$\rho_0(t,x) \approx \sum \bar{\rho}_i(t)\,\delta\left(x-\bar{x}_i(t)\right), \tag{2}$$

where $\bar{x}_i$ is the location of a concentration point and $\bar{\rho}_i$ is the weight of each concentration. A more precise description of such concentration profiles is the real phase WKB ansatz -or Hopf–Cole transform- as introduced in [3, 23] for studying traveling fronts, when a better accuracy is kept introducing a microscale ε. The leading idea is similar to the Dirac mass approximating the Gaussian

$$\delta(x-\bar{x}) \approx \frac{1}{\sqrt{2\pi\,\varepsilon}}\exp\frac{-|x-\bar{x}|^2}{2\varepsilon} = \exp\frac{-|x-\bar{x}|^2-\varepsilon 2\pi\,\ln(\varepsilon)}{2\varepsilon}.$$

Therefore, the method relies on the Hopf–Cole transform

$$\rho_\varepsilon(t,x) = \exp^{-\frac{\phi_\varepsilon(t,x)}{\varepsilon}}, \qquad \lim_{\varepsilon\to 0}\phi_\varepsilon \geqslant 0,$$

where ε is a small positive parameter determining a specific regime, typically of high frequencies, in which there may be formation of concentrations and patterns, where the concentration points are understood as the minima of the phase ϕ_ε. This kind of analysis typically leads, in the limit $\varepsilon\to 0$, to a constrained Hamilton–Jacobi equation for the phase $\phi_0\geqslant 0$, to be understood by *viscosity solutions* [18]. Such a Hamilton–Jacobi equation enables to determine the correct concentration profile ϕ_ε. It has been developed in the framework of adaptive dynamics, [4, 19, 29, 31, 32], where it also allows to derive the so-called canonical equation for the evolution of the maxima of ϕ_0 which here represents the fittest trait in a structured population rather than the concentration points of a population density. Specifically, on the maxima points $\bar{x}_i$ we have that $\phi_0=0$, and in the limit $\varepsilon\to 0$ the macroscopic density ρ_0 can be written as (2).

In the context of kinetic equations, the major difficulty is to find the Hamiltonian, and this has been first achieved by Bouin and Calvez in [7]. They study a kinetic model with a BGK relaxation operator with a homogeneous kernel, leading to a homogeneous constant steady equilibrium ρ^∞. In a high frequency regime, they use the Hopf–Cole transform of the distribution

$$f_\varepsilon(t,x,v,\hat{v}) = \exp^{-\frac{\varphi_\varepsilon(t,x,v,\hat{v})}{\varepsilon}} \tag{3}$$

and also, following celebrated paper [20], use the perturbed test function $\varphi_\varepsilon(t,x,v,\hat{v}) = \varphi(t,x)+\varepsilon\eta(t,x,v,\hat{v})$, i.e. the leading order in ε only depends on (t,x). In order to state a large deviation principle, the authors in [7] built the Hamiltonian and in the limit $\varepsilon\to 0^+$ a Hamilton–Jacobi equation to which the phase φ_0 is a viscosity solution. This has been extended in higher space dimensions in [10] where new difficulties may occur as the 'dimensionality problem' and lack of $\mathcal{C}^1$ regularity for the Hamiltonian. In [5, 6, 9] the authors study

front propagation in transport-reaction kinetic equations. In [8] the authors study a BGK type equation in a high frequency regime and with a spatially homogeneous Maxwellian with vanishing variance and derive a new constrained nonlocal Hamilton–Jacobi equation.

In the present work, we analyse the concentration profile for the solutions of kinetic equations of the class (1) as introduced in [34, 36]. These use a BGK-like kernel T with the specificity to be spatially nonhomogenous and nonlocal. Following, [7], we build the Hamiltonian in the real phase WKB method and present a new method to deal with inhomogeneity and circumvent the 'dimensionality problem' in this context. Differently with respect to [7], our aim is to study the concentration profiles by means of an appropriate Hamilton–Jacobi equation, in the same spirit as in adaptive dynamics models. Specifically, we want to prove that the distribution f converges to a *concentration solution* that is in the form

$$f_0(t,x,v,\hat{v}) = \sum \omega_i \delta(x-\bar{x}_i), \tag{4}$$

with weights $\omega_i(v,\hat{v})$ and $\bar{x}_i$ being the minimum points of the phase, corresponding to $\varphi(\bar{x}_i)=0$, as in (3). Interestingly enough, the classical diffusion approximation of (1) does not characterise correctly the concentration profile and just generates the eikonal equation, i.e. a second order approximation of the true Hamiltonian.

In the first section, we present the nonlocal kinetic equation under study along with the local and nonlocal rescalings that we consider in order to derive evolution equations for the aggregate quantities -the so-called macroscopic or hydrodynamic equations- that we revise in the appendix A. As a preparation before studying the nonlinear case, we study in section 2 a linear case in which the kernel T depends on an assigned external signal $\mathcal{S}$. Specifically, we perform the real phase WKB analysis of the linear nonlocal equation and present the concentration result as well as the canonical equation for the evolution of the maxima and some examples along with numerical tests. The analysis of the linear case allows to connect the results obtained by means of the analysis performed with the WKB ansatz to a more classical hydrodynamic analysis of the kinetic equation, but shows that it also allows to explain concentration profiles and to locate the maximum points. section 3 is devoted to the nonlinear case, when the nonhomogeneous nonlocal kernel T depends on ρ. Here the classical hydrodynamic is far from allowing to understand the full portrait of the concentration profiles. We extend formally the WKB analysis and a striking novel feature is a convex-concave Hamiltonian which takes into account low density instability, in accordance with the linear instability criteria derived in previous works [36]. It allows us to explain the saw tooth profile of the concentrations. In section 4, we draw some conclusions.

1. Preliminaries

1.1. A nonlocal kinetic equation

In the same spirit as [34], we consider the kinetic equation (1) with transition probability that depends on the external signal $\mathcal{S}:\Omega\to\mathbb{R}_+$, that is measured nonlocally in the physical space and that affects the choice of the direction of the cells. The turning operator $T[\mathcal{S}](v,\hat{v})$ is a probability on $\mathcal{V}$, depending on x through $\mathcal{S}$. It is defined by

$$T[\mathcal{S}](v,\hat{v}) = c(x)\,\psi(v|\hat{v})\,b(\mathcal{S}(x+R\hat{v})), \qquad c(x)^{-1} := \int_{\mathbb{S}^{d-1}} b(\mathcal{S}(x+R\hat{v}))\,\mathrm{d}\hat{v}, \tag{5}$$

where $b(\cdot)$ is a function that weights the external field $\mathcal{S}$, while the quantity R is the sensing radius defining the neighborhood where the cell measures the field $\mathcal{S}$. The function

$\psi : [0,U] \to \mathbb{R}_+$ is the distribution of the possible speeds $v \in [0,U]$ on a given direction $\hat{v}$, satisfying

$$\int_0^U \psi(v|\hat{v})\,\mathrm{d}v = 1 \quad \forall \hat{v} \in \mathbb{S}^{d-1}.$$

We denote its average speed (along direction $\hat{v}$) V_ψ and second statistical moment D^2_ψ (that we assume to be independent of the direction), i.e. they are defined by

$$V_\psi(\hat{v}) := \int_0^U \psi(v|\hat{v})\, v\,\mathrm{d}v, \qquad D^2_\psi := \int_0^U \psi(v|\hat{v})\, v^2\,\mathrm{d}v. \tag{6}$$

These properties ensure that $T[\mathcal{S}](v,\hat{v})$ is a probability density function on $\mathcal{V} = [0,U] \times \mathbb{S}^{d-1}$ as

$$\int_{\mathcal{V}} T[\mathcal{S}](v,\hat{v})\,\mathrm{d}\hat{v}\mathrm{d}v = 1,$$

in such a way that the number density is conserved at (t,x). In other words, the balance equation holds

$$\partial_t \rho(t,x) + \nabla_x \cdot \int_{\mathcal{V}} f(t,x,v,\hat{v})\, v\hat{v}\mathrm{d}\hat{v}\mathrm{d}v = 0. \tag{7}$$

Then, we can also define the average velocity of the transition probability $T[\mathcal{S}]$ as

$$\mathbf{U}_{\mathcal{S}}(x) = \int_{\mathcal{V}} T[\mathcal{S}](v,\hat{v})\,\mathbf{v}\,\mathrm{d}\hat{v}\mathrm{d}v, \tag{8}$$

and its variance-covariance matrix

$$\mathbb{D}_{\mathcal{S}}(x) = \int_{\mathcal{V}} T[\mathcal{S}](v,\hat{v})\,(\mathbf{v}-\mathbf{U}_{\mathcal{S}}) \otimes (\mathbf{v}-\mathbf{U}_{\mathcal{S}})\,\mathrm{d}\hat{v}\mathrm{d}v. \tag{9}$$

We remark that, when Ω is bounded, in order to deal with the boundary, we must restrict the sensing radius using the formula

$$R(x,\hat{v}) := \min\{\lambda \in [0,R] : x + \lambda\hat{v} \in \Omega\}. \tag{10}$$

Equation (1) needs to be coupled with initial and boundary conditions, defined by, respectively

$$f(0,x,v,\hat{v}) = f^0(x,v,\hat{v}), \qquad (x,v,\hat{v}) \in \Omega \times [0,U] \times \mathbb{S}^{d-1}, \tag{11}$$

$$f(t,x,v,\hat{v}) = \mathcal{R}\left[f_{|\Gamma_+}\right](t,x,v,\hat{v}) \qquad x \in \partial\Omega,\, v \in [0,U],\, \hat{v} \in \Gamma_-(x), \tag{12}$$

where

$$\Gamma_\pm(x) := \{\hat{v} \in \mathbb{S}^{d-1} : \hat{v} \cdot \boldsymbol{n}(x) \gtrless 0\},$$

with $\boldsymbol{n}(x)$ the outward normal to the boundary $\partial\Omega$ in the point x. As boundary conditions for the kinetic equation, we assume a standard diffusive boundary condition [30, 40] called Maxwellian boundary conditions, defined as

$$\mathcal{R}[f_+](t,x,v,\hat{v}) = \alpha(x) f(t,x,v,\mathcal{W}(\hat{v})) + (1-\alpha(x)) M(x,v,\hat{v}) \times \int_0^U \int_{\hat{v}^*\cdot \boldsymbol{n}\geqslant 0} f(t,x,v^*,\hat{v}^*)\,|\hat{v}^*\cdot \boldsymbol{n}|\mathrm{d}\hat{v}^*\mathrm{d}v^*, \tag{13}$$

where $\mathcal{W}(\hat{v}) = -\hat{v}$ for the bounce back reflection condition and $\mathcal{W}(\hat{v}) = \hat{v} - 2(\hat{v}\cdot \boldsymbol{n})\boldsymbol{n}$ for the specular reflection. Diffusive boundary conditions are no-flux boundary conditions at the macroscopic level [40], in the sense that the total population density is conserved in Ω, and we normalise it as

$$\int_\Omega \rho(t,x)\,\mathrm{d}x = \int_\Omega \int_{\mathcal{V}} f(t,x,v,\hat{v})\,\mathrm{d}\hat{v}\,\mathrm{d}v\,\mathrm{d}x = 1, \qquad \forall t \geqslant 0. \tag{14}$$

In fact, it may be proved, see [40], that a solution f to (1)-(11)-(12)-(13) satisfies the no-flux condition

$$\int_{\mathcal{V}} f(t,x,v,\hat{v})\,\mathbf{v}\cdot\mathbf{n}(x)\,\mathrm{d}\hat{v}\,\mathrm{d}v = 0, \quad \forall x\in\partial\Omega, \quad t>0. \tag{15}$$

The equilibrium distribution of (1) is given by

$$f^\infty(x,v,\hat{v}) = \rho^\infty(x)\,T[\mathcal{S}](v,\hat{v}).$$

As $T[\mathcal{S}]$ depends on x through $\mathcal{S}$, in order for f^∞ to be a stationary equilibrium, then the following must be satisfied

$$-\frac{\mathbf{v}\cdot\nabla_x\rho^\infty}{\rho^\infty} = \frac{\mathbf{v}\cdot\nabla_x T[\mathcal{S}]}{T[\mathcal{S}]}, \tag{16}$$

showing that ρ^∞ is not always the constant homogeneous solution, being $T[\mathcal{S}]$ space dependent because of the spatial heterogeneity of $\mathcal{S}$ and of the nonlocality. With classical arguments (Jensen's inequality) and assuming Maxwellian boundary conditions (that are nonabsorbing boundary conditions [12]) it is easy to see that given a convex function Φ, then

$$\frac{\mathrm{d}}{\mathrm{d}t}\int_\Omega\int_{\mathcal{V}} \Phi\left(f(t,x,v,\hat{v})\right)\mathrm{d}v\mathrm{d}\hat{v}\mathrm{d}x \leqslant 0,$$

and the equality holds if and only if $f = f^\infty$. This equilibrium is asymptotically stable and does not depend on the initial condition.

1.2. Rescaling

We now consider a regime in which reorientations occur at random exponential times with rate $\mu = \dfrac{1}{\varepsilon}$, i.e. the dynamics is ruled by

$$\partial_t f_\varepsilon(t,x,v,\hat{v}) + \mathbf{v}\cdot\nabla_x f_\varepsilon(t,x,v,\hat{v}) = \frac{1}{\varepsilon}\left(\rho_\varepsilon(t,x)\,T[\mathcal{S}]_\varepsilon(v,\hat{v}) - f_\varepsilon(t,x,v,\hat{v})\right), \tag{17}$$

where the limit $\varepsilon\to 0$ defines a high frequency regime, i.e. many reorientations are happening in the time unit, in such a way the system reaches the equilibrium quickly. In (17), $T[\mathcal{S}]_\varepsilon(v,\hat{v})$ is to be understood as a rescaled transition probability in the regime defined by ε. We now

explain that this regime can be interpreted in (at least) two opposite ways due to the presence of the nonlocality.

A first possible interpretation is to see equation (17) as the result of a hyperbolic scaling of equation (1) defined by

$$(t,v,x) \to \left(\frac{t}{\varepsilon}, v, \frac{x}{\varepsilon}\right). \tag{18}$$

The latter, in the same spirit of geometric optics, defines a macroscopic (or large) space scale and a long time scale that is needed for observing significant phenomena in order to compensate for the macroscopic space scale. The long time scale is actually needed in order to reach the equilibrium defined by interactions happening with a frequency 1 in the time unit. In this macroscopic space scale interactions are localised, as one needs to consider a scaling of the sensing radius R, i.e.

$$R \to \varepsilon R,$$

that naturally leads to a localisation of the interactions of the cells with the background $\mathcal{S}$. In this sense the large scale limit of (17) for $\varepsilon \to 0$ leads to the hydrodynamic (fluid) behavior of the system on a macroscopic space scale that must be observed on a long time scale.
However, *a priori* we can consider the perspective of the following classical nondimensionalisation

$$x \to \frac{x}{L}, \quad t \to \frac{t}{t_0}, \quad v \to \frac{v}{V}, \quad \rho \to \frac{\rho}{\bar{\rho}}, \quad f \to \frac{f}{\bar{\rho}/V^d}, \quad T[\mathcal{S}] \to \frac{T[\mathcal{S}]}{V^d}, \tag{19}$$

where t_0 and L are characteristic time and length scales of the system, V is the typical speed, while $\bar{\rho}$ is a reference density. Plugging (19) in (1) we obtain

$$\mathrm{St}\,\partial_t f(t,x,v,\hat{v}) + \mathbf{v}\cdot\nabla_x f(t,x,v,\hat{v}) = \frac{1}{\mathrm{Kn}}\left(\rho(t,x)\,T[\mathcal{S}](v,\hat{v}) - f(t,x,v,\hat{v})\right), \tag{20}$$

where the kinetic Strouhal number St and Knudsen number Kn are defined as

$$\mathrm{St} := \frac{L}{Vt_0}, \qquad \mathrm{Kn} := \frac{V}{L\mu}.$$

The regime under consideration in (17) corresponds to having parameters satisfying

$$\mathrm{St} \sim \mathcal{O}(1), \qquad \mathrm{Kn} \sim \mathcal{O}(\varepsilon) \ll 1. \tag{21}$$

By looking at (20) we observe that the parameters regime (21) corresponds to a large time horizon t_0 satisfying

$$t_0 \sim \frac{\varepsilon^{-1}}{\mu}, \tag{22}$$

where $\sim$ is, here and in the following, to be meant as a quantitative statement, regardless of the units. This may be rephrased saying that we choose ε such that

$$\frac{V}{L} \sim \mathcal{O}(\varepsilon), \tag{23}$$

and we choose a drift long time scale as

$$t_0 = \frac{L}{V},$$

that satisfies (22) because of (23). We remark that if $V = \mathcal{O}(1)$, then $\dfrac{1}{L} \sim \varepsilon$, that amounts to (18) (where we use again $R \to \varepsilon R$).

Conversely, a second possible interpretation is $L = \mathcal{O}(1)$, i.e. we observe the dynamics on the *microscopic* space scale, then (23) amounts to a regime of very small speeds $V \sim \varepsilon$ that must be observed, in order to balance the smallness of the speed, on a long time scale. This can be seen as a scaling in the form

$$(t, v, x) \to \left(\frac{t}{\varepsilon}, \varepsilon v, x\right). \tag{24}$$

The latter may also be seen as a nonlocal regime as the sensing radius R is not rescaled.

2. Concentration profile and the Hamilton–Jacobi equation

We want to study the concentration profile of the solution f_ε of equation (17) by studying the equation for a phase φ_ε obtained through the Hopf–Cole transform (3). We expect that $\varphi_\varepsilon(t,x,v,\hat{v})$ behaves quadratically, and thus that $f_\varepsilon(t,x,v,\hat{v})$ behaves like a Dirac mass near each concentration point, giving rise in the limit $\varepsilon \to 0$ to a concentration profile in the form (4). For this reason, we study the limit of φ_ε.

2.1. Derivation of the Hamilton–Jacobi equation

At first we remark that, from equation (17), φ_ε satisfies the equation

$$\partial_t \varphi_\varepsilon + \mathbf{v}\cdot\nabla_x\varphi_\varepsilon = 1 - T[\mathcal{S}]_\varepsilon(v,\hat{v}) \int_{\mathcal{V}} \exp\frac{-\varphi_\varepsilon(t,x,w,\hat{w}) + \varphi_\varepsilon(t,x,v,\hat{v})}{\varepsilon}\, \mathrm{d}w\mathrm{d}\hat{w}. \tag{25}$$

From this we get

$$(1 - \partial_t\varphi_\varepsilon - \mathbf{v}\cdot\nabla_x\varphi_\varepsilon) = T[\mathcal{S}]_\varepsilon(v,\hat{v}) \int_{\mathcal{V}} \exp\frac{-\varphi_\varepsilon(t,x,w,\hat{w}) + \varphi_\varepsilon(t,x,v,\hat{v})}{\varepsilon}\, \mathrm{d}w\mathrm{d}\hat{w}. \tag{26}$$

Following [7, 29], we may also look for f_ε under the form

$$f_\varepsilon(t,x,v,\hat{v}) = Q_\varepsilon(t,x,v,\hat{v}) \exp^{-\frac{\tilde{\varphi}_\varepsilon(t,x)}{\varepsilon}}, \qquad \varphi_\varepsilon(t,x,v,\hat{v}) = \tilde{\varphi}_\varepsilon(t,x) - \varepsilon \ln Q_\varepsilon(t,x,v,\hat{v}), \tag{27}$$

with $\tilde{\varphi}_\varepsilon$ and Q_ε to be determined. Furthermore, we may normalise them as

$$\int_{\mathcal{V}} Q_\varepsilon(t,x,v,\hat{v})\, \mathrm{d}\hat{v}\mathrm{d}v = 1, \qquad \forall t \geqslant 0,\ x \in \Omega,$$

which, thanks to (7), implies

$$\int_\Omega \exp^{-\frac{\tilde{\varphi}_\varepsilon(t,x)}{\varepsilon}} \mathrm{d}x = 1, \qquad \forall t \geqslant 0.$$

Setting

$$p_\varepsilon := \nabla_x \tilde{\varphi}_\varepsilon, \qquad H_\varepsilon := -\partial_t \tilde{\varphi}_\varepsilon, \tag{28}$$

we can write equation (26) as

$$\begin{aligned} &\varepsilon\left[\partial_t Q_\varepsilon(t,x,v,\hat{v}) + \mathbf{v}\cdot\nabla_x Q_\varepsilon(t,x,v,\hat{v})\right] + (1 + H_\varepsilon - v\hat{v}\cdot p_\varepsilon) Q_\varepsilon(t,x,v,\hat{v}) \\ &\quad = T[\mathcal{S}]_\varepsilon(v,\hat{v}) \int_{\mathcal{V}} Q_\varepsilon(t,x,w,\hat{w})\,\mathrm{d}\hat{w}\mathrm{d}w. \end{aligned} \tag{29}$$

Considering the (formal at this stage) common limit of φ_ε or $\tilde{\varphi}_\varepsilon$

$$\varphi := \lim_{\varepsilon\to 0^+} \tilde{\varphi}_\varepsilon,$$

the (formal) limit as $\varepsilon \to 0$ gives us $Q_\varepsilon(t,x,w,\hat{w}) \to \mathcal{Q}(x,\nabla_x\varphi(t,x),v,\hat{v})$, with

$$\begin{cases} (1 + H - v\hat{v}\cdot p)\,\mathcal{Q}(x,p,v,\hat{v}) = T[\mathcal{S}]_0(v,\hat{v}) \int_{\mathcal{V}} \mathcal{Q}(x,p,w,\hat{w})\,\mathrm{d}\hat{w}\mathrm{d}w, \\ \mathcal{Q}(x,p,v,\hat{v}) \geqslant 0, \qquad \int_{\mathcal{V}} \mathcal{Q}(x,p,v,\hat{v})\,\mathrm{d}\hat{v}\mathrm{d}v = 1 \quad \forall p,\ x \in \Omega. \end{cases} \tag{30}$$

This is an eigenvalue-eigenfunction problem in $(v,\hat{v})$, with parameters (t,x). Thanks to the Krein–Rutman theory, see [28], with good properties of $T[\mathcal{S}]_0$ to be discussed later, this eigenproblem has a unique solution. The eigenvalue H is solely determined by the parameters p and $\mathcal{S}(x)$ and we can write $H = H(x,p)$ which provides us with the Hamilton–Jacobi equation for the dominant term in (28)

$$\partial_t\varphi + H(x,\nabla_x\varphi) = 0. \tag{31}$$

Notice that we can expect that the problem (29) itself has a particular solution $Q_\varepsilon(t,x,v,\hat{v})$ similar to the *principal bundle*, see [28, 29], for parabolic equations. It is similar to a time dependent eigenvalue problem. Up to our knowledge this notion has never been studied for kinetic equations.

These formal conclusions rely on the possibility to define a smooth Hamiltonian $H(x,p)$, a question we analyse now.

2.2. The effective Hamiltonian

As in [7], one can characterise the eigenvalue $H(x,p)$ arising in equation (30), rewriting it as

$$\mathcal{Q}(x,p,v,\hat{v}) = \frac{T[\mathcal{S}]_0(v,\hat{v}) \int_{\mathcal{V}} \mathcal{Q}(x,p,w,\hat{w})\,\mathrm{d}\hat{w}\mathrm{d}w}{1 + H(x,p) - v\hat{v}\cdot p} > 0. \tag{32}$$

We remind that $H(x,p)$ also depends explicitly on x as $T[\mathcal{S}]_0$ depends on x. Integrating with respect to $v,\hat{v}$ and using the normalisation in equation (30), we obtain the problem

$$\text{find } H \text{ such that:} \qquad 1 = \int_{\mathcal{V}} \frac{T[\mathcal{S}]_0(v,\hat{v})}{1 + H(x,p) - v\hat{v}\cdot p}\,\mathrm{d}v\mathrm{d}\hat{v}. \tag{33}$$

In particular we obviously have

$$1 = \int_{\mathcal{V}} \frac{T[\mathcal{S}]_0(v,\hat{v})}{1+H(x,0)}\,\mathrm{d}v\mathrm{d}\hat{v}, \qquad H(x,0) = 0.$$

Equation (33) can be uniquely solved by strict monotonicity in H and also gives that

$$-U|p| < H(x,p) < U|p|,$$

because $|v| \leqslant U$ and when $H = U|p|$ the denominator is larger than 1 for all $(v,\hat{v})$ and when $H = -U|p|$ the denominator is smaller than 1.

However these bounds are not enough to compute from this Hamiltonian a positive eigenfunction $\mathcal{Q}$. As observed in [10], it is necessary to introduce some further assumption; this is the so-called 'dimensionality problem', because the difficulty only occurs when $d \geqslant 2$. The values of H for which the denominator in (33) vanishes are given by:

$$\underline{H}(p) = -1 + \max_{\mathcal{V}} \left[v\hat{v}\cdot p\right].$$

We then introduce a new assumption, which simplifies and generalises to heterogeneous Hamiltonians that of [10], that is

$$\inf_x \int_{\mathcal{V}} \frac{T[\mathcal{S}]_0(v,\hat{v})}{1+\underline{H}(p) - v\hat{v}\cdot p}\,\mathrm{d}v\mathrm{d}\hat{v} > 1. \tag{34}$$

The latter ensures that $H(x,p) > \underline{H}(p)$, and thus that the denominator, and therefore $\mathcal{Q}$, are positive for the solution of equation (33). In dimension $d = 1$, the integral in (33) would blow up if the denominator vanishes, therefore the condition is always satisfied. In higher dimension this restriction is needed.

Additionally, differentiating (33) in p, we find

$$0 = \int_{\mathcal{V}} \frac{T[\mathcal{S}]_0(v,\hat{v})\left(\nabla_p H(x,p) - v\hat{v}\right)}{\left(1+H(x,p) - v\hat{v}\cdot p\right)^2}\,\mathrm{d}v\mathrm{d}\hat{v}.$$

We now look for the extremal values of the Hamiltonian, as we want to study the long time equilibria of the system. Specifically, we want to see when the uniform steady state (corresponding to $p = \nabla_x\varphi \equiv 0$) is a possible equilibrium or, conversely, when formation of concentration solutions occurs for large times. Concentration solutions are related to a macroscopic density ρ that displays maxima, that correspond to minima points of φ. It means, therefore, points $\bar{x}_i$ such that $\nabla_x\varphi(\bar{x}_i) = 0$. In general, when $p = \nabla_x\varphi = 0$ we have that, using the definition (8), we get

$$\nabla_p H(x,0) = \mathbf{U}^0_{\mathcal{S}}(x), \tag{35}$$

which, in general, does not vanish, as already argued, as $T[\mathcal{S}]_0$ is not in principle symmetric as a function of $\hat{v}$, as instead assumed in [7]. Moreover, differentiating twice, we find

$$\int_{\mathcal{V}} \frac{T[\mathcal{S}]_0(v,\hat{v})\,D^2_p H(p)}{\left(1+H(p) - v\hat{v}\cdot p\right)^2}\,\mathrm{d}v\mathrm{d}\hat{v} = 2\int_{\mathcal{V}} \frac{T[\mathcal{S}]_0(v,\hat{v})\left(\nabla_p H(p) - v\hat{v}\right)\otimes\left(\nabla_p H(p) - v\hat{v}\right)}{\left(1+H(p) - v\hat{v}\cdot p\right)^3}\,\mathrm{d}v\mathrm{d}\hat{v},$$

and then we have that $D^2_p H$ is positive definite as (34) holds. We may also compute

$$D^2_p H(x,0) = 2\mathbb{D}_{\mathcal{S}}(x), \tag{36}$$

that is positive definite being the variance-covariance matrix of a positive transition probability. Then, in order to characterise the configuration $p = 0$ and to discriminate between constant solutions and concentrations, the dependency of H on x and p is crucial. If $\mathbf{U}_{\mathcal{S}}(x) \equiv 0$, then $\nabla_p H(x,0) \equiv 0$, and the constant solution is a minimum point of H and no concentration occurs. Else, when $\mathbf{U}_{\mathcal{S}}(x) = \nabla_p H(x,0)$ is not identically 0, there may be concentration solutions that, at the stationary state for large times t_f, possibly with $t_f = \infty$, display aggregations in the points $\bar{x}_i$ such that $p(\bar{x}_i) = \nabla_x \varphi(\bar{x}_i) = 0$ and $\nabla_p H(\bar{x}_i, 0) = \mathbf{U}^0_{\mathcal{S}}(\bar{x}_i) = 0$. In conclusion, the points $(\bar{x}_i, 0)$ that are stationary points of the average of the transition probability $T[\mathcal{S}]_0$, are the minima points of H and concentration solutions around those points are stable equilibria for large times.

2.3. The concentration result

To simplify, we work in the full space, $\Omega = \mathbb{R}^d$. We assume that the initial condition φ^0_ε defined on $\Omega \times \mathcal{V}$ satisfies uniformly in ε

$$\begin{cases} |\nabla_x \varphi^0_\varepsilon| \in L_\infty(\Omega \times \mathcal{V}), \qquad \varphi^0_\varepsilon(x,v,\hat{v}) = \tilde{\varphi}^0(x) + O(\varepsilon), \\ \partial_t \varphi_\varepsilon(t=0) := -\mathbf{v} \cdot \nabla_x \varphi^0_\varepsilon + 1 \\ \qquad -T[\mathcal{S}]_\varepsilon(v,\hat{v}) \displaystyle\int_{\mathcal{V}} \exp \frac{-\varphi^0_\varepsilon(x,w,\hat{w}) + \varphi^0_\varepsilon(x,v,\hat{v})}{\varepsilon} \, \mathrm{d}w\mathrm{d}\hat{w} \in L_\infty(\Omega \times \mathcal{V}), \end{cases} \tag{37}$$

$$\int_{\mathbb{R}^d \times \mathcal{V}} f^0_\varepsilon(x,v,\hat{v}) \, \mathrm{d}x\mathrm{d}v\mathrm{d}\hat{v} = 1, \qquad \int_{\mathbb{R}^d \times \mathcal{V}} |x| f^0_\varepsilon(x,v,\hat{v}) \, \mathrm{d}x\mathrm{d}v\mathrm{d}\hat{v} \quad \text{is bounded}, \tag{38}$$

and for some constants $T_- > 0$, $L_M > 0$

$$\begin{cases} T[\mathcal{S}]_\varepsilon \geqslant T_- > 0, \qquad T[\mathcal{S}]_\varepsilon + |\nabla_x T[\mathcal{S}]_\varepsilon| + |\nabla_{\mathbf{v}} T[\mathcal{S}]_\varepsilon| \leqslant L_M, \\ T[\mathcal{S}]_\varepsilon \to T[\mathcal{S}]_0 \quad \text{uniformly}. \end{cases} \tag{39}$$

Then we can prove the

Theorem 1. *We make the assumptions (34) and (37)–(39). Then, after extractions,*

(i) *φ_ε is uniformly (in ε) bounded and Lipschitz (locally in time),*
(ii) *φ_ε converges locally uniformly on $\mathbb{R}_+ \times \mathbb{R}^d \times \mathcal{V}$ toward $\varphi \geqslant 0$ where φ does not depend on $v, \hat{v}$. Moreover, φ is the viscosity solution of the Hamilton–Jacobi equation (31) with initial condition $\varphi^0(x)$ and with a convex in p for each fixed x Hamiltonian $H(x,p)$ uniquely implicitly determined by the formula (33),*
(iii) *f_ε converges weakly to a measure f supported by the non-empty set $\{\varphi = 0\}$.*

Remark. 1. The set $\{\varphi = 0\}$ is included in the $\{x \in \Omega : H(x,0) = 0\}$ and therefore is typically discrete.
2. Compared to [7], the kernel $T[\mathcal{S}]_\varepsilon$ depends on x, which is an additional major technical difficulty. Also a difference here is the ε dependency in $T[\mathcal{S}]_\varepsilon$ which we circumvent with our assumptions.
3. The author in [10] faces the difficulty of gradient estimates as here. He argues by limsup-liminf arguments which optimises the assumptions. Here we do not go to this elaborate method and use simpler arguments based on Lipschitz estimates.

4. The corrector satisfies, according to the Hopf–Cole transform (27), approximately $\mathcal{Q}_\varepsilon = \dfrac{f_\varepsilon}{\rho_\varepsilon}$. However, we also have that $\dfrac{f_\varepsilon}{\rho_\varepsilon} \to T[\mathcal{S}]_0$ and $\mathcal{Q}_\varepsilon \to \mathcal{Q}$ when ε tends to zero. Actually, thanks to (30), we find

$$\mathcal{Q}(x,0,v,\hat{v}) = T[\mathcal{S}]_0(v,\hat{v}). \tag{40}$$

5. When Ω is bounded, we impose no-flux boundary conditions (15). Therefore, considering (27), we have

$$\exp^{-\frac{\tilde{\varphi}_\varepsilon}{\varepsilon}} \int_{\mathcal{V}} Q_\varepsilon(t,x,v,\hat{v})\, v\hat{v}\cdot\boldsymbol{n}\, \mathrm{d}v\mathrm{d}\hat{v} = 0, \qquad x \in \partial\Omega,$$

and thus

$$\int_{\mathcal{V}} Q_\varepsilon(t,x,v,\hat{v})\, v\hat{v}\cdot\boldsymbol{n}\, \mathrm{d}v\mathrm{d}\hat{v} = 0, \qquad x \in \partial\Omega,$$

and, in the limit $\varepsilon \to 0^+$, we complete the eigenproblem (30) with the no-flux condition

$$\int_{\mathcal{V}} \mathcal{Q}(x,p,v,\hat{v})\, v\hat{v}\cdot\boldsymbol{n}\, \mathrm{d}v\mathrm{d}\hat{v} = 0, \qquad x \in \partial\Omega. \tag{41}$$

It would be interesting to investigate if this relation can be interpreted as a Neumann boundary condition on $p = \nabla_x\varphi$. Remark that for small p, Taylor expanding $\mathcal{Q}$ defined in (32) as a function of p about $p = 0$, remembering (40) and plugging the expression into (41), we find

$$[\mathbf{U}^0_{\mathcal{S}} + \mathbb{D}^0_{\mathcal{S}}\nabla_x\varphi]\cdot\boldsymbol{n} = 0. \tag{42}$$

Proof. When the proof uses standard arguments, see for instance [2, 18], we only sketch them. We begin with *a priori* estimates (i) for the solution of equation (25). From assumption (37), we infer

$$|\partial_t\varphi_\varepsilon(t,x,v,\hat{v})| \leqslant |\partial_t\varphi^0_\varepsilon(x,v,\hat{v})| \leqslant C,$$

(we do not prove it because we detail the case of space derivatives which are more involved), therefore

$$|\varphi_\varepsilon(t,x,v,\hat{v})| \leqslant |\varphi^0_\varepsilon(x,v,\hat{v})| + Ct.$$

Also, still using the maximum principle for derivatives and the already proved bounds (here equation (25) is used again for x-derivative of $T[\mathcal{S}]$), we have that

$$\sum_{i=1}^d |\partial_i\varphi_\varepsilon(t,x,v,\hat{v})| \leqslant \sum_{i=1}^d |\partial_i\varphi^0_\varepsilon(x,v,\hat{v})|\,\mathrm{e}^{Ct} + Ct.$$

Since this estimate is more elaborate, we prove it. Differentiating equation (25) in x_i and setting $\psi_i = \partial_i\varphi_\varepsilon(t,x,v,\hat{v})$, we find

$$\partial_t\psi_i + \mathbf{v}\cdot\nabla\psi_i = -T[\mathcal{S}]_\varepsilon \int_{\mathcal{V}} \exp\frac{-\varphi_\varepsilon(t,x,w,\hat{w}) + \varphi_\varepsilon(t,x,v,\hat{v})}{\varepsilon}\,\frac{\psi_i(v,\hat{v}) - \psi_i(w,\hat{w})}{\varepsilon}\,\mathrm{d}w\mathrm{d}\hat{w} + \mathrm{RHS}$$

where the RHS term is

$$\mathrm{RHS} = \partial_t T[\mathcal{S}]_\varepsilon(v,\hat{v}) \int_{\mathcal{V}} \exp \frac{-\varphi_\varepsilon(t,x,w,\hat{w}) + \varphi_\varepsilon(t,x,v,\hat{v})}{\varepsilon} \,\mathrm{d}w\mathrm{d}\hat{w}.$$

Using again equation (25), it can be estimated as

$$\begin{aligned}|\mathrm{RHS}| &\leqslant \frac{|\partial_t T[\mathcal{S}]_\varepsilon(v,\hat{v})|}{T[\mathcal{S}]_\varepsilon(v,\hat{v})} T[\mathcal{S}]_\varepsilon(v,\hat{v}) \int_{\mathcal{V}} \exp \frac{-\varphi_\varepsilon(t,x,w,\hat{w}) + \varphi_\varepsilon(t,x,v,\hat{v})}{\varepsilon} \,\mathrm{d}w\mathrm{d}\hat{w} \\ &= \frac{|\partial_t T[\mathcal{S}]_\varepsilon(v,\hat{v})|}{T[\mathcal{S}]_\varepsilon(v,\hat{v})} \left[1 - \partial_t \varphi_\varepsilon - \mathbf{v}\cdot\nabla\varphi_\varepsilon\right],\end{aligned}$$

and, using the assumption (39) and the time derivative estimate, we conclude that

$$|\mathrm{RHS}| \leqslant C + C\sum_{j=1}^{d} |\psi_j|.$$

With this observation, we can use the maximum principle for $\psi_i \mathrm{e}^{-Ct} + C$ and conclude the bounds on the x derivatives.

With these estimates, we conclude that for $t \leqslant \tilde{T}$, we have

$$\int_{\mathcal{V}} \exp \frac{-\varphi_\varepsilon(t,x,w,\hat{w}) + \varphi_\varepsilon(t,x,v,\hat{v})}{\varepsilon} \,\mathrm{d}w\mathrm{d}\hat{w} \leqslant C\left(\tilde{T}\right),$$

which can be written

$$\varphi_\varepsilon(t,x,v,\hat{v}) = \varepsilon \ln \int_{\mathcal{V}} \exp \frac{-\varphi_\varepsilon(t,x,w,\hat{w})}{\varepsilon} \,\mathrm{d}w\mathrm{d}\hat{w} + O(\varepsilon).$$

This tells us that a limit of φ_ε depends only on (t,x). As in [7], it also gives directly the last estimate of (i), that is

$$|\partial_{\mathbf{v}}\varphi_\varepsilon(t,x,v,\hat{v})| \leqslant \left[|\partial_x \varphi_\varepsilon^0(x,v,\hat{v})| + |\partial_{\mathbf{v}}\varphi_\varepsilon^0(x,v,\hat{v})|\right] \mathrm{e}^{Ct} + Ct.$$

We are now in the same situation as [7] and the rest of the argument follows in a similar way. Using the perturbed test function method, [20], we obtain the statement (ii) thanks to the assumption (34) which allows us to define $\mathcal{Q}$ and avoid the 'dimensionality problem'.

Finally, for the statement (iii), we notice that the mass conservation is immediate which implies that $\varphi(t,x) \leqslant 0$. Then, we observe that

$$\frac{\mathrm{d}}{\mathrm{d}t}\int_{\mathbb{R}^d\times\mathcal{V}} |x| f_\varepsilon(t,x,v,\hat{v})\,\mathrm{d}x\mathrm{d}v\mathrm{d}\hat{v} \leqslant \int_{\mathbb{R}^d\times\mathcal{V}} |\mathbf{v}| f_\varepsilon(t,x,v,\hat{v})\,\mathrm{d}x\mathrm{d}v\mathrm{d}\hat{v} \leqslant U.$$

Therefore f_ε is a tight probability measure and, after extraction, it converges weakly to a probability measure which implies that $\min_{x\in\Omega}\varphi(t,x) = 0$ for all $t \geqslant 0$. The only possible concentration points are when $\varphi(t,x)$ is zero (see [4, 19, 32] for details and consequences). □

2.4. The Hamilton–Jacobi formalism and hydrodynamics

The Hamilton–Jacobi equation (31) also arises in the more classical hydrodynamic limits (see appendix A), and also allows to describe the concentration profiles. We investigate the relation with respect to the characterisation of concentration solutions in the two regimes, kinetic one and hydrodynamic one.

2.4.1. An eikonal equation. Given the hydrodynamic expansion (76), where we keep a small diffusion term, the phase $\phi_\varepsilon = -\varepsilon \log \rho_\varepsilon$ satisfies, in the limit $\varepsilon \to 0^+$, the Hamilton–Jacobi equation

$$\partial_t \phi + \mathbf{U}^0_{\mathcal{S}} \cdot \nabla \phi + \nabla_x \phi^T \mathbb{D}^0_{\mathcal{S}} \nabla_x \phi = 0. \tag{43}$$

When working in a bounded domain, from (77), we additionally obtain the boundary condition

$$\left[\mathbf{U}^0_{\mathcal{S}} + \mathbb{D}^0_{\mathcal{S}} \nabla_x \phi\right] \cdot \boldsymbol{n} = 0. \tag{44}$$

As φ satisfies (31) and ϕ satisfies (43), we conclude, as observed in [7], that the two procedures (aggregate quantities limit and WKB analysis) do not commute in general as far as concentration profiles are concerned. This is because the Hilbert or Chapman–Enskog expansions leading to the hydrodynamic limits are additive, while the Hopf–Cole transform that leads to (31) is multiplicative. However, equation (43) corresponds to the quadratic expansion of the Hamiltonian H from (31) in a neighborhood of $\nabla_x \phi = 0$ remembering (35)–(36), and thus describes the same concentration effects but not the correct kinetic profiles. Actually, the boundary conditions (44) for the eikonal equation (43) are the same as (42) that were obtained for (31) in the limit of small p.

It is also possible to detect a regime in which the kinetic Hamiltonian will converge to the eikonal one. Consider the regime (81) or (83), corresponding to (82) or (84), and the assumption of small diffusivity (85). Then, considering $\rho_\nu = \exp^{-\frac{\phi}{\nu}}$ and letting $\nu \to 0$, Equation (82) becomes

$$\partial_t \phi + \mathbf{U}_{\mathcal{S}} \cdot \nabla_x \phi + \nabla_x \phi^T \bar{\mathbb{D}}_{\mathcal{S}} \nabla_x \phi = 0, \tag{45}$$

while equation (84) becomes

$$\partial_t \phi + + \mathbf{U}^1_{\mathcal{S}} \cdot \nabla_x \phi + \nabla_x \phi^T \bar{\mathbb{D}}^0_{\mathcal{S}} \nabla_x \phi = 0. \tag{46}$$

We now consider

$$\varepsilon \to \varepsilon \nu,$$

and plug (3) in (80); in the limit $\varepsilon \to 0$, we obtain

$$\partial_t \left(\left[\frac{\varphi}{\nu} \right] \right) + H_\nu \left(\nabla_x \left[\frac{\varphi}{\nu} \right] \right) = 0, \tag{47}$$

where H_ν is implicitly defined by

$$1 = \nu \int_{\mathcal{V}} \frac{T[\mathcal{S}]_0(v, \hat{v})}{\nu + H_\nu(x,p) - v\hat{v} \cdot p} \, \mathrm{d}v \mathrm{d}\hat{v}, \quad p = \nabla_x \left[\frac{\varphi}{\nu} \right].$$

Then, as $D^2H(0)=\dfrac{2}{\nu^2}\mathbb{D}^0_{\mathcal{S}}$, considering ν small and assuming the small diffusivity (85), we obtain

$$H(x,\nabla_x\varphi)=H(x,0)+\nabla_x\varphi\cdot\nabla_pH(x,0)+\frac{1}{2}\nabla_x\varphi^T D_p^2H(x,0)\,\nabla_x\varphi=\mathbf{U}^0_{\mathcal{S}}\cdot\nabla_x\varphi+\nabla_x\varphi^T\mathbb{D}^0_{\mathcal{S}}\nabla_x\varphi\,.$$

Plugging the latter in (47) allows to obtain the equivalent form of equation (43).

Let us now consider a spatially homogeneous T such that

$$\int_{\mathcal{V}}T\mathrm{d}v\mathrm{d}\hat{v}=1,\qquad\int_{\mathcal{V}}Tv\mathrm{d}v\mathrm{d}\hat{v}=0,\qquad\int_{\mathcal{V}}Tv^2\hat{v}\otimes\hat{v}\,\mathrm{d}v\mathrm{d}\hat{v}=\nu^2\mathbb{I}.$$

It is the case for example, in one-dimension, where $\mathcal{V}=[-U,U]$, and we choose $T=\exp^{-\dfrac{v^2}{2}}$, $T=\dfrac{1}{U}$, or $T=\dfrac{1}{2}\left(\delta(v-U)+\delta(v+U)\right)$, see [7]. Then, performing the WKB analysis leads to (47) and, then, to $\partial_t\varphi+|\nabla^2_x\varphi|=0$, while, starting from (87) we obtain $\partial_t\phi+|\nabla^2_x\phi|=0$, that is (46) with $\mathbf{U}^1_{\mathcal{S}}=0$. We highlight, in fact, that in these cases there is no correction term $T[\mathcal{S}]_1$ (and then no $\mathbf{U}^1_{\mathcal{S}}$). In conclusion, the two procedures commute in the regime of small ν.

Interestingly, in the case

$$T[\mathcal{S}]=c\,(x)\,\mathcal{S}\,(x+R\hat{v})\,,$$

considering (24) or (81) and a large R, the two procedures lead to (45) and (82), respectively. Conversely, if we consider a small R and $T[\mathcal{S}]_0, T[\mathcal{S}]_1$ as defined as a consequence of a localised scaling (83), we obtain (84) with $\mathbb{D}^0_{\mathcal{S}}=\mathbb{I}$, $\mathbf{U}^1_{\mathcal{S}}=R\dfrac{\nabla_x\mathcal{S}}{\mathcal{S}}$. If in the WKB analysis we consider (18), we obtain the eikonal equation $\partial_t\varphi+|\nabla^2_x\varphi|=0$ and the higher order effect is naturally lost in the localised hyperbolic scaling.

2.4.2. Dynamics of the concentration points. We now want to recover the dynamics of the concentration points. For this we look for the trajectory $\bar{x}_i(t)$ of the maximum (or concentration) points of ρ. In the context of adaptive dynamics, this is interpreted as the 'fittest trait', [4, 19, 29, 32]. In the Hopf–Cole transform in the limit $\varepsilon\to 0$, the concentration points are defined by the minimum points $\bar{x}_i$ of $\varphi\geqslant 0$, i.e.

$$\varphi\,(t,\bar{x}_i\,(t))=0,\qquad\nabla_x\varphi\,(t,\bar{x}_i\,(t))=0,\qquad\partial_t\varphi\,(t,\bar{x}_i\,(t))=0=H\left(\bar{x}_i\,(t)\,,0\right),\tag{48}$$

and

$$D^2_x\varphi\,(t,\bar{x}_i\,(t))\geqslant 0.$$

First of all, we remark that in the regime (17) for $\varepsilon\to 0$, the hydrodynamics allow us to state that each trajectory in the physical space (see (78)) follows the differential equation

$$\dot{x}\,(t)=\mathbf{U}^0_{\mathcal{S}}\,(x(t))\,.\tag{49}$$

If $T[\mathcal{S}]_0$ is space homogeneous (e.g. $b(\mathcal{S})=\mathcal{S}$ in the regime (18)), then we know from the kinetic equation (1) that the homogeneous configuration ρ^∞ is the asymptotic stationary equilibrium. Then, the Hamilton–Jacobi formalism allows to state that if $\mathbf{U}^0_{\mathcal{S}}(x(t))=0\,\forall x$ then

$\nabla_x\varphi \equiv 0$ being a minimum of H, and, thus, the constant solution is the asymptotic equilibrium configuration. Conversely, in the regime (24) in general $\mathbf{U}^0_{\mathcal{S}}(x(t))$ does not vanish and the maxima points of ρ (the concentration points) are the minima points of φ that are defined as $\bar{x}_i(t) : \mathbf{U}_{\mathcal{S}}(\bar{x}_i(t)) = 0$. Therefore, from (49) $\dot{\bar{x}}_i(t) = 0$ and this tells us that the maxima points $\bar{x}_i$ of ρ do not evolve in time. We now want to verify how the Hamilton–Jacobi equation can be exploited in order to describe the time evolution of the concentration points. In order to do this, we derive a canonical equation in the same spirit as in [4, 19, 29, 32]. Differentiating with respect to time the second equality on (48) (that is along the trajectories), we find

$$0 = \frac{\mathrm{d}}{\mathrm{d}t}\nabla_x\varphi\left(t,\bar{x}_i\left(t\right)\right) = \partial_t\nabla_x\varphi\left(t,\bar{x}_i\left(t\right)\right) + \dot{\bar{x}}_i D_x^2\varphi\left(t,\bar{x}_i\left(t\right)\right).$$

Also, differentiating (31) with respect to x, we get

$$\partial_t\nabla_x\varphi\left(t,\bar{x}_i\right) = -\nabla_x H\left(x,\nabla_x\varphi\left(t,x\right)\right) - \nabla_p H\left(x,\nabla_x\varphi\left(t,x\right)\right).D_x^2\varphi\left(t,x\right),$$

and, specialising it in $\bar{x}_i(t)$, and remembering (35) and $H(x,0) = 0$, we get

$$\partial_t\nabla_x\varphi\left(t,\bar{x}_i\left(t\right)\right) = -\nabla_p H\left(x,\nabla_x\varphi\left(t,\bar{x}_i\right)\right)\cdot D_x^2\varphi\left(t,\bar{x}_i\right) = -\mathbf{U}^0_{\mathcal{S}}\left(\bar{x}_i\left(t\right)\right)\cdot D_x^2\varphi\left(t,\bar{x}_i\right).$$

Therefore we obtain

$$\dot{\bar{x}}_i\left(t\right) = \mathbf{U}^0_{\mathcal{S}}\left(\bar{x}_i\left(t\right)\right),$$

that is the same as (49), specialised on the concentration points. In particular the long term limit is solely determined by $\mathbf{U}^0_{\mathcal{S}}$ and does not depend on the initial condition of ρ as it is usual in adaptive dynamics, and as it follows from the H-Theorem in kinetic theory, that establishes in this linear case that the equilibrium is asymptotically stable and does not depend on the initial condition.

Therefore, the steady state concentration points occur and are defined by the set

$$\Omega_M := \{\bar{x}_i, i = 1,\ldots,n : \varphi\left(\bar{x}_i\right) = 0\} \subset \{\bar{x}_i, i = 1,\ldots,m : \mathbf{U}^0_{\mathcal{S}}\left(\bar{x}_i\right) = 0\}. \tag{50}$$

As a consequence of theorem 1, concentration solutions have support in Ω_M and specifically are in the form (4) with

$$\omega_i\left(x,v,\hat{v}\right) = \rho\left(\bar{x}_i\right)\mathcal{Q}\left(\bar{x}_i,p\left(\bar{x}_i\right),v,\hat{v}\right), \tag{51}$$

where

$$\mathcal{Q}\left(\bar{x}_i,p\left(\bar{x}_i\right),v,\hat{v}\right) = T\left[\mathcal{S}\right]_0\left(v,\hat{v}\right)_{|x=\bar{x}_i}, \tag{52}$$

remembering $p(\bar{x}_i) = 0$ and (40). From the eikonal equation we may expect that

$$\rho_0\left(t,x\right) = \sum \frac{\rho^\infty}{\det \mathbb{D}^0_{\mathcal{S}}\left(\bar{x}_i\right)}\delta\left(x-\bar{x}_i\right),$$

so that $\rho(\bar{x}_i) = \dfrac{\rho^\infty}{\det \mathbb{D}^0_{\mathcal{S}}(\bar{x}_i)}$.

In conclusion, in the linear case the hydrodynamics and the Hamilton–Jacobi equations give the same amount of information regarding the evolution of the concentration points, but the Hamilton–Jacobi formalism allows to characterise the concentration points and profiles. When the zeroes of $\mathbf{U}^0_{\mathcal{S}}$ are discrete, the generic situation, the long term solution must be concentrated as Dirac masses on these points. Else if $\mathbf{U}^0_{\mathcal{S}}$ is identically zero, then no concentrations are observed in the long run.

2.5. Examples

We illustrate the results with two examples in one dimension. We first choose the signal

$$\mathcal{S}(x) = \mathcal{S}_0 \exp^{-\frac{(x-\bar{x})^2}{2\sigma^2}}, \tag{53}$$

with $\bar{x}$ a given point in Ω. When $b(\mathcal{S}) = \mathcal{S}$, it generates a transition probability given by

$$T[\mathcal{S}](v,\hat{v}) = \psi(v|\hat{v}) \frac{\exp^{-\frac{R(x-\bar{x})\cdot\hat{v}}{2\sigma^2}}}{\int_{\mathbb{S}^{d-1}} \exp^{-\frac{R(x-\bar{x})\cdot\hat{v}}{2\sigma^2}} \mathrm{d}\hat{v}}.$$

Firstly, we remark that the characteristic length of variation of $\mathcal{S}$, that can be defined as in (86), is given by

$$l_{\mathcal{S}} = \frac{\sigma^2}{\max|x-\bar{x}|}.$$

In the regime (24), we expect that the maximum point $\mathbf{U}^0_{\mathcal{S}}(x(t)) = 0$ only occurs when $x(t) = \bar{x}$. Moreover, we expect a unique nonhomogeneous stationary state whose profile needs to satisfy (16). In the regime (18), conversely, as the limiting $T[\mathcal{S}]_0$ does not depend on x, we expect that the homogeneous configuration is the stationary equilibrium, as $\partial_t \rho = 0$. We now consider the Hopf–Cole analysis. In 1D we have that $\hat{v} = \pm 1$ and choosing $\psi(v|\hat{v}) = \delta(v - V)$ with $V, R = \mathcal{O}(1)$ we get

$$H(x,p) = \frac{1}{2}\frac{V^2p^2 + Vp\mathcal{D}_{\mathcal{S}}(x)}{1+\sqrt{1+4V^2p^2-4Vp\mathcal{D}_{\mathcal{S}}(x)}}, \qquad \mathcal{D}_{\mathcal{S}}(x) = \frac{\exp^{\frac{R(x-\bar{x})}{2\sigma^2}} - \exp^{-\frac{R(x-\bar{x})}{2\sigma^2}}}{\exp^{\frac{R(x-\bar{x})}{2\sigma^2}} + \exp^{-\frac{R(x-\bar{x})}{2\sigma^2}}}. \tag{54}$$

We remark that in the regime (18), in (3) (and, then, in (54)) R is to be replaced with εR, and, hence, the Hamiltonian vanishes only in $p = 0$ and every concentration disappears as $\nabla_p H(x,0) \equiv 0$. Conversely, in the regime (24), the Hamiltonian has two different zeros $p(x) = 0, \frac{\mathcal{D}_{\mathcal{S}}(x)}{V}$. Specifically, now the minimum point of H is $(\bar{x}, \frac{\mathcal{D}_{\mathcal{S}}(\bar{x})}{V})$. As a consequence, the concentration solution of the Hamilton–Jacobi equation is

$$\varphi(x) = \frac{1}{V}\int \mathcal{D}_{\mathcal{S}}(z)\,\mathrm{d}z = \frac{\sigma^2}{RV}\log\left|\cosh\left(\frac{R}{\sigma^2}(x-\bar{x})\right)\right| \tag{55}$$

that is depicted in figure 1(first line, second panel).

We numerically solve equation (1). The numerical method adopted here is the same used in the works [34–36]. A first order splitting is performed: the space transport is numerically solved by means of an explicit finite-difference Van-Leer scheme, while the relaxation step is performed implicitly, thanks to the BGK-like structure. We consider $\Omega = [0,1]$, $\mu = 1$ and $V = 5\cdot 10^{-5}$ and $\psi(v) = \frac{1}{2V}$. In all simulations the space grid has a uniform mesh defined by

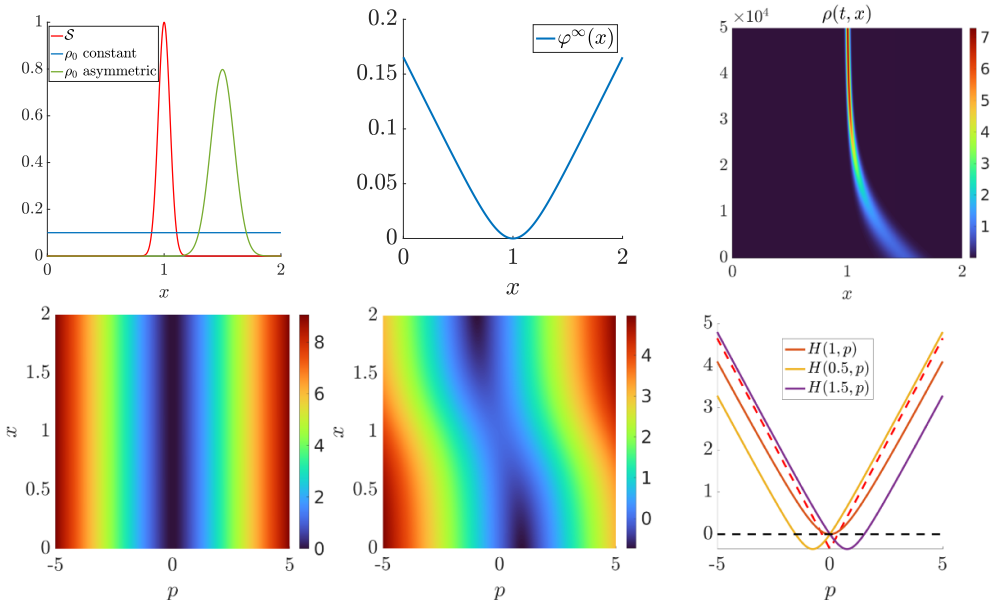

Figure 1. First line. First panel: $\mathcal{S}$ (red curve) given by (53) and two different initial conditions ρ^0: the constant one (blue) and an asymmetric Gaussian (green). Second panel: solution (55) of the Hamilton–Jacobi equation. Third panel: temporal evolution of $\rho(t,x)$ in the case of an asymmetric ρ^0. Second line. First panel: $H(x,p)$ (54) in the local regime (18), second and third panel: $H(x,p)$ (54) in the nonlocal regime (24). In the third panel the red dashed lines correspond to $\pm U|p|$, while the black horizontal dashed line indicates the level zero.

$\mathrm{d}x = 10^{-3}$. In figure 1 we use $\mathcal{S}$ given by (53) with $\sigma = 0.05$ and $\bar{x} = 1$, $R = 0.01$. Therefore $l_{\mathcal{S}} = 5 \cdot 10^{-3}$. Let us consider $L = 1$. We are then in regime (24) with $\varepsilon = 10^{-5}$. We consider two different initial conditions $\rho^0 = 0.1$ and ρ^0 Gaussian centered in 1.5. As already mentioned the stationary state is unique and does not depend on the initial condition. In the second line of Fig 1, second and third panel, we plot the Hamiltonian (54). We remark that the Hamiltonian is not always positive and there is a concentration profile. Specifically, the Hamiltonian is not uniformly convex with respect to x as a function of p. Conversely, in a regime defined by $V = 5 \cdot 10^{-5}$, $L = l_{\mathcal{S}}$ (i.e. regime (18) with $\varepsilon = 10^{-2}$) the stationary state ρ_∞ is the stationary homogeneous configuration even for a nonhomogeneous initial condition (not shown), and this is true in both regimes $R \lesseqgtr l_{\mathcal{S}}$. The corresponding Hamiltonian is plotted in figure 1, second line, first panel, and it is a convex function with respect to p forall x.

Second, we choose a bimodal signal

$$\mathcal{S}(x) = \mathcal{S}_1 \exp^{-\frac{(x-\tilde{x}_1)^2}{2\sigma_1^2}} + \mathcal{S}_2 \exp^{-\frac{(x-\tilde{x}_2)^2}{2\sigma_2^2}}. \tag{56}$$

Then the number of singular points $\bar{x}_i$ satisfying $\mathbf{U}_{\mathcal{S}}(\bar{x}_i) = 0$ depends on R, $\tilde{x}_1 - \tilde{x}_2$ and on σ^2. In figure 2 we consider the bimodal signal $\mathcal{S}$ given by (56) with $\sigma_1 = \sigma_2 = 0.03$ and three different couples of $\tilde{x}_1, \tilde{x}_2$ according to the value of their distance with respect to $R = 0.4$. Here again $\varepsilon = 10^{-5}$ (same values of V, L, μ). We remark that, when $\tilde{x}_2 - \tilde{x}_1 \leqslant R$ (see figure 2(b) for the case $\tilde{x}_2 - \tilde{x}_1 = R$), then there is a single peak as $\exists!\ \bar{x}_1 (= 0)$ such that $\mathbf{U}_{\mathcal{S}}(\bar{x}_1) = 0$. The

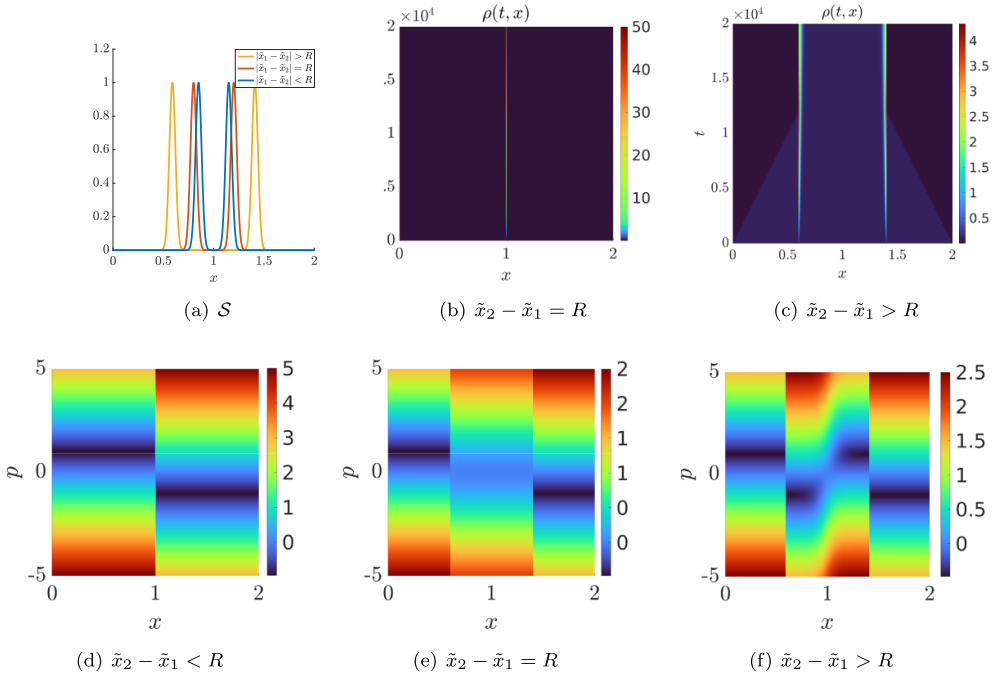

(a) $\mathcal{S}$ (b) $\tilde{x}_2 - \tilde{x}_1 = R$ (c) $\tilde{x}_2 - \tilde{x}_1 > R$

(d) $\tilde{x}_2 - \tilde{x}_1 < R$ (e) $\tilde{x}_2 - \tilde{x}_1 = R$ (f) $\tilde{x}_2 - \tilde{x}_1 > R$

Figure 2. Temporal evolution of $\rho(t,x)$ in case of $\mathcal{S}$ given by (56). Here $R = 0.4$, the initial condition ρ^0 is constant. In (a): three different $\mathcal{S}$ as given by (56) with $\sigma_1 = \sigma_2 = 0.03$ and three different couples of $\tilde{x}_2, \tilde{x}_1$. In (b)–(c) temporal evolution of $\rho(t,x)$ for the two different $\mathcal{S}$: in (b) $\tilde{x}_2 - \tilde{x}_1 = R$, in (c) $\tilde{x}_2 - \tilde{x}_1 > R$. In (d)–(f) we plot the Hamiltonian for the three different cases.

case $\tilde{x}_2 - \tilde{x}_1 < R$ behaves like $\tilde{x}_2 - \tilde{x}_1 = R$ (not shown). When $\tilde{x}_2 - \tilde{x}_1 > R$ (see figure 2(c)) then $\exists\, \bar{x}_1, \bar{x}_2$ such that $\mathbf{U}_{\mathcal{S}}(\bar{x}_i) = 0$, $i = 1,2$. In figure 2(d) we plot the Hamiltonian in the case $\tilde{x}_2 - \tilde{x}_1 > R$.

In figure 3 we consider $\mathcal{S}$ given by (56) with $\sigma_1 = 2\sigma_2, \sigma_2 = 0.03$ while for the sensing radius we have again $R = 0.4$. We consider two different couples of $\tilde{x}_1, \tilde{x}_2$ as shown in figure 3(a). We remark that the peaks of ρ do not coincide with the peaks of $\mathcal{S}$ and this is due to the nonlocality ($R > 0$). In particular, in the first case (b) the distance between the maxima of $\mathcal{S}$ is larger than the sensing radius and, thus, the stationary solution has two peaks even though with different convexity due to the configuration of $\mathcal{S}$. In the second case (c), the distance between the peaks of $\mathcal{S}$ is exactly $R/2$, so that the peak of the stationary solution is unique, even though it is asymmetric, because of the asymmetry of $\mathcal{S}$.

In conclusion, in this linear case the analysis of the kinetic equations and of the aggregate limits by means of the hydrodynamics give almost a complete set of information concerning the dynamics of the maxima, except the concentration result and the location of the maxima, for which the WKB analysis is needed. Therefore, we now consider a nonlinear case in which the study of the kinetic and hydrodynamic equations may not be able to convey all the necessary information regarding the dynamics of the maxima points, while the Hamilton–Jacobi formalism offers promising tools in order to describe the concentration profiles.

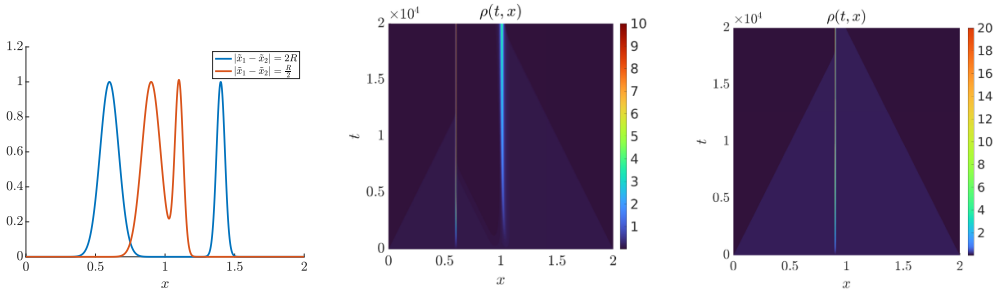

(a) $\mathcal{S}$ (b) $\tilde{x}_2 - \tilde{x}_1 = 2R$ (c) $\tilde{x}_2 - \tilde{x}_1 = R/2$

Figure 3. Temporal evolution of $\rho(t,x)$ in case of $\mathcal{S}$ given by (56). Here $R = 0.4$ and $\sigma_1 = 0.06, \sigma_2 = 0.03$. In (a): two different $\mathcal{S}$ given by (56) with two different couples $\tilde{x}_2, \tilde{x}_1$. In (b) and (c) the corresponding time evolution of the densities ρ.

3. A nonlinear case

When the external field affecting the reorientation choice is the cell density itself, i.e. $\mathcal{S} = \rho$, then the kinetic equation (1) becomes nonlinear

$$\partial_t f(t,x,v,\hat{v}) + \mathbf{v}\cdot\nabla_x f(t,x,v,\hat{v}) = \mu\left(\rho(t,x)\,T[\rho](v,\hat{v}) - f(t,x,v,\hat{v})\right), \tag{57}$$

where, given the specific choice $b(\rho) = \rho$, the tumbling operator is defined as

$$T[\rho] = \frac{\rho(t,x+R\hat{v})}{\int_{\mathbb{S}^{d-1}} \rho(t,x+R\hat{v})\,\mathrm{d}\hat{v}}\psi(v|\hat{v}). \tag{58}$$

The latter describes the tendency of cells, that is typical in cell-cell adhesion, of migrating towards regions $x + R\hat{v}$ -and therefore of reorienting along direction $\hat{v}$- in which the cell density is higher. Other cell-cell adhesion mechanisms may be taken into account, by modulating the choice of b [36]. In [36] the authors perform a linear stability analysis of the kinetic model (57) and (58). In the one dimensional case $d = 1$ and with the choice $\psi(v|\hat{v}) = \delta(v - V_\psi(\hat{v}))$, they show that the uniform homogeneous configuration is stable if, using the notation (6),

$$\frac{V}{R\mu} > 1, \qquad V := \frac{V_\psi(+1) + V_\psi(-1)}{2}. \tag{59}$$

We now consider regime (18), and in this nondimensionalised regime $V, R, \mu = \mathcal{O}(1)$, then equation (57) reads

$$\frac{\partial f_\varepsilon}{\partial t}(t,x,v,\hat{v}) + \mathbf{v}\cdot\nabla_x f_\varepsilon(t,x,v,\hat{v}) = \frac{\mu}{\varepsilon}\left(\rho_\varepsilon T[\rho]_\varepsilon - f_\varepsilon(t,x,v,\hat{v})\right), \tag{60}$$

where

$$T[\rho]_\varepsilon = \frac{\rho_\varepsilon(t,x+\varepsilon R\hat{v})}{\int_{\mathbb{S}^{d-1}} \rho_\varepsilon(t,x+\varepsilon R\hat{v})\,\mathrm{d}\hat{v}}\psi(v|\hat{v}).$$

In particular, in the rescaled regime (18), relation (59) is unchanged since

$$\frac{\varepsilon V}{R\varepsilon\mu} = \frac{V}{R\mu}.$$

With $\mathbf{U}_\rho^\varepsilon$ and $\mathbb{D}_\rho^\varepsilon$ defined thanks to (8) and (9), the hydrodynamic expansion is given by

$$\partial_t \rho_\varepsilon + \nabla_x \cdot \left(\mathbf{U}_\rho^\varepsilon \rho_\varepsilon\right) = \frac{\varepsilon}{\mu} \nabla_x \cdot \nabla_x \cdot \left(\mathbb{D}_\rho^\varepsilon \rho_\varepsilon + \rho_\varepsilon \mathbf{U}_\rho^\varepsilon \nabla_x \cdot \mathbf{U}_\rho^\varepsilon\right). \tag{61}$$

When ρ_ε is smooth enough, the limiting transition probability becomes

$$\lim_{\varepsilon \to 0} T[\rho]_\varepsilon = T[\rho]_0 := \frac{1}{|\mathbb{S}^{d-1}|} \psi(v|\hat{v}).$$

3.1. Derivation of the Hamilton–Jacobi equation

When ρ_ε undergoes concentration, we may consider (3), and write

$$\begin{aligned} T[\rho]_\varepsilon &= \psi(v|\hat{v}) \frac{\int_{\mathcal{V}} \exp\left(-\dfrac{\varphi_\varepsilon(t, x+\varepsilon R\hat{v}, w, \hat{w})}{\varepsilon}\right) \mathrm{d}w\mathrm{d}\hat{w}}{\int_{\mathbb{S}^{d-1}} \int_{\mathcal{V}} \exp\left(-\dfrac{\varphi_\varepsilon(t, x+\varepsilon R\hat{v}, w, \hat{w})}{\varepsilon}\right) \mathrm{d}w\mathrm{d}\hat{w}\mathrm{d}\hat{v}} \\ &\approx \psi(v|\hat{v}) \frac{\int_{\mathcal{V}} \exp\left(\dfrac{-\varphi_\varepsilon(t,x,w,\hat{w}) - \varepsilon R\hat{v}\cdot\nabla_x\varphi_\varepsilon(t,x,w,\hat{w})}{\varepsilon}\right) \mathrm{d}w\mathrm{d}\hat{w}}{\int_{\mathcal{V}} \int_{\mathbb{S}^{d-1}} \exp\left(-\dfrac{\varphi_\varepsilon(t,x,w,\hat{w}) + \varepsilon R\hat{v}\cdot\nabla_x\varphi_\varepsilon(t,x,w,\hat{w})}{\varepsilon}\right) \mathrm{d}w\mathrm{d}\hat{w}\,\mathrm{d}\hat{v}}, \end{aligned}$$

where we have used the expansion

$$\varphi_\varepsilon(t, x+\varepsilon R\hat{v}, w, \hat{w}) = \varphi_\varepsilon(t,x,w,\hat{w}) + \varepsilon R\hat{v}\cdot\nabla_x\varphi_\varepsilon(t,x,w,\hat{w}).$$

Then, assuming (27), and remembering that $\tilde{\varphi}_\varepsilon$ does not depend on $v, \hat{v}$, we have

$$T[\rho]_\varepsilon \approx \psi(v|\hat{v}) \frac{\exp\left(\dfrac{-\tilde{\varphi}_\varepsilon(t,x)}{\varepsilon}\right) \exp^{-R\hat{v}\cdot\nabla_x\tilde{\varphi}_\varepsilon(t,x)} \int_{\mathcal{V}} Q_\varepsilon \,\mathrm{d}w\mathrm{d}\hat{w}}{\exp\left(\dfrac{-\tilde{\varphi}_\varepsilon(t,x)}{\varepsilon}\right) \int_{\mathbb{S}^{d-1}} \int_{\mathcal{V}} Q_\varepsilon \mathrm{d}w\mathrm{d}\hat{w} \exp^{-R\hat{v}\cdot\nabla_x\tilde{\varphi}_\varepsilon}\,\mathrm{d}\hat{v}},$$

thanks to the Fubini–Tonelli theorem. Then, letting $\varepsilon \to 0^+$, we obtain

$$T[\rho]_\varepsilon \to G_R(v, \hat{v}, \nabla_x\varphi) = \psi(v|\hat{v}) \frac{\exp^{-R\hat{v}\cdot\nabla_x\varphi}}{\displaystyle\int_{\mathbb{S}^{d-1}} \exp^{-R\hat{v}\cdot\nabla_x\varphi}\,\mathrm{d}\hat{v}}, \tag{62}$$

that is the approximation of the transition probability defined by the Hopf–Cole transform in the regime (18).

Plugging (3) in (60) we obtain

$$\mu - \partial_t\varphi_\varepsilon - \mathbf{v}\cdot\nabla_x\varphi_\varepsilon = \exp\left(\frac{\varphi_\varepsilon(t,x,v,\hat{v})}{\varepsilon}\right) \frac{\mu}{\varepsilon} \left[\int_{\mathcal{V}} \exp\left(-\frac{\varphi_\varepsilon(t,x,w,\hat{w})}{\varepsilon}\right) \mathrm{d}w\mathrm{d}\hat{w}\, T[\rho]_\varepsilon\right].$$

Furthermore, considering the expansion (27), and by letting (formally) ε go to 0^+, we obtain

$$\mu - \partial_t\varphi - \mathbf{v}\cdot\nabla_x\varphi = \mu\left[Q^{-1}(x,v,\hat{v})\int_{\mathcal{V}} Q(x,w,\hat{w})\,\mathrm{d}w\mathrm{d}\hat{w}G_R(v,\hat{v},\nabla_x\varphi)\right]. \tag{63}$$

Again, we assume that $Q(x,w,\hat{w})$ is positive according to assumption (34). Then, like in the previous section, we define an eigenvalue-eigenvector problem

$$(\mu + H(p) - v\hat{v}\cdot p)\,\mathcal{Q}(p,v,\hat{v}) = \mu G_R(v,\hat{v},p)\int_{\mathcal{V}}\mathcal{Q}(p,w,\hat{w})\,\mathrm{d}w\mathrm{d}\hat{w}.$$

We remark that the term G_R results from the interaction kernel T and arises due to the nonlocal sensing of ρ. As such, its role is to drive the dynamics of f toward the equilibrium in $v,\hat{v}$. We remark that it satisfies:

$$\nabla_p G_R(v,\hat{v},p) = \psi(v|\hat{v})\left[\frac{-R\hat{v}\exp^{-R\hat{v}\cdot p}}{\int_{\mathbb{S}^{d-1}}\exp^{-R\hat{w}\cdot p}\,\mathrm{d}\hat{w}} + \frac{\exp^{-R\hat{v}\cdot p}R\int_{\mathbb{S}^{d-1}}\exp^{-R\hat{w}\cdot p}\,\hat{w}\,\mathrm{d}\hat{w}}{\left(\int_{\mathbb{S}^{d-1}}\exp^{-R\hat{w}\cdot p}\,\mathrm{d}\hat{w}\right)^2}\right],$$

and, then

$$G_R(v,\hat{v},0) = \frac{\psi(v|\hat{v})}{|\mathbb{S}^{d-1}|}, \qquad \nabla_p G_R(v,\hat{v},0) = -\psi(v|\hat{v})\frac{R}{|\mathbb{S}^{d-1}|}\hat{v}.$$

From (63), we find that the (formal) limit φ is the solution of

$$\partial_t\varphi + H(\nabla_x\varphi) = 0, \tag{64}$$

where the Hamiltonian is implicitly defined by

$$1 = \mu\int_{\mathcal{V}}\frac{G_R(v,\hat{v},p)}{\mu + H(p) - v\hat{v}\cdot p}\,\mathrm{d}v\mathrm{d}\hat{v}. \tag{65}$$

We remark that now H only depends on p and not on x, and this is because we are considering the localised regime (18). It is easy to see that $H(0) = 0$. Then, by differentiating (65) with respect to p we obtain

$$0 = \mu\int_{\mathcal{V}}\frac{\nabla_p G_R(v,\hat{v},p)}{(\mu + H(p) - v\hat{v}\cdot p)}\,\mathrm{d}v\mathrm{d}\hat{v} - \mu\int_{\mathcal{V}}\frac{G_R(v,\hat{v},p)\,(\nabla_p H(p) - v\hat{v})}{(\mu + H(p) - v\hat{v}\cdot p)^2}\,\mathrm{d}v\mathrm{d}\hat{v}.$$

Therefore $\nabla_p H(p) = \mathbf{U}_R^G(p)$, where $\mathbf{U}_R^G$ is the average of G_R, i.e.

$$\mathbf{U}_R^G(p) = \int_{\mathcal{V}} G_R(v,\hat{v},p)\,v\hat{v}\,\mathrm{d}v\mathrm{d}\hat{v} = \frac{\int_{\mathbb{S}^{d-1}} V_\psi(\hat{v})\exp^{-R\hat{v}\cdot p}\,\hat{v}\mathrm{d}\hat{v}}{\int_{\mathbb{S}^{d-1}} V_\psi(\hat{v})\exp^{-R\hat{v}\cdot p}\,\mathrm{d}\hat{v}}, \tag{66}$$

so that

$$\nabla_p H(0) = \mathbf{U}_R^G(0) = \int_{\mathbb{S}^{d-1}} V_\psi(\hat{v})\,\hat{v}\,\mathrm{d}\hat{v}. \tag{67}$$

We remark that $\nabla_p H(0)$ vanishes in the case in which V_ψ is even.

Differentiating further, the Hessian of H satisfies

$$\int_{\mathcal{V}} \frac{G_R(v,\hat{v},p)\,D^2H(p)}{(\mu+H-v\hat{v}p)^2}\,\mathrm{d}v\mathrm{d}\hat{v} = 2\int_{\mathcal{V}} \frac{G_R\,(\nabla_p H - v\hat{v})\otimes(\nabla_p H - v\hat{v})}{(\mu+H-v\hat{v}p)^3}\,\mathrm{d}v\mathrm{d}\hat{v} + \int_{\mathcal{V}} \frac{D_p^2 G_R}{\mu+H-v\hat{v}p}\,\mathrm{d}v\mathrm{d}\hat{v} - 2\int_{\mathcal{V}} \frac{\nabla_p G_R\,(\nabla_p H - v\hat{v})}{(\mu+H-v\hat{v}p)^2}\,\mathrm{d}v\mathrm{d}\hat{v}.$$

We have $D_p^2 G_R(v,\hat{v},0) = 0$ because

$$D_p^2 G_R\,(v,\hat{v},p) = \psi\,(v|\hat{v})\,R^2\exp^{-R\hat{v}\cdot p}\left[\frac{\hat{v}\otimes\hat{v}}{\int_{\mathbb{S}^{d-1}}\exp^{-R\hat{v}\cdot p}\,\mathrm{d}\hat{v}} - 2\frac{\hat{v}\otimes\int_{\mathbb{S}^{d-1}}\exp^{-R\hat{v}\cdot p}\,\hat{v}\,\mathrm{d}\hat{v}}{\left(\int_{\mathbb{S}^{d-1}}\exp^{-R\hat{v}\cdot p}\,\mathrm{d}\hat{v}\right)^2} - \frac{\int_{\mathbb{S}^{d-1}}\exp^{-R\hat{v}\cdot p}\,\hat{v}\otimes\hat{v}\,\mathrm{d}\hat{v}}{\left(\int_{\mathbb{S}^{d-1}}\exp^{-R\hat{v}\cdot p}\,\mathrm{d}\hat{v}\right)^2} + 2\frac{\int_{\mathbb{S}^{d-1}}\exp^{-R\hat{v}\cdot p}\,\hat{v}\,\mathrm{d}\hat{v}\otimes\int_{\mathbb{S}^{d-1}}\exp^{-R\hat{v}\cdot p}\,\hat{v}\,\mathrm{d}\hat{v}}{\left(\int_{\mathbb{S}^{d-1}}\exp^{-R\hat{v}\cdot p}\,\mathrm{d}\hat{v}\right)^3}\right].$$

Then, in the case in which ψ does not depend on $\hat{v}$, we have $V = V_\psi$ and

$$D_p^2 H(0) = \frac{2dD_\psi^2}{\mu}\mathbb{I} - 2\mathrm{d}vR\mathbb{I} = 2d\left(\frac{D_\psi^2}{\mu} - VR\right)\mathbb{I} \tag{68}$$

that is positive definite when

$$\frac{D_\psi^2}{V} > R\mu. \tag{69}$$

If the latter holds, then the homogeneous steady state $p \equiv 0$ is a minimum of the Hamiltonian, and it is, thus, the asymptotic equilibrium. Conversely, $p = 0$ is a (possibly local) maximum point of the Hamiltonian. As for $p \to \pm\infty$, $H \to \infty$, and if H is C^1, we then expect nonvanishing minima points $\bar{p}$ of the Hamiltonian that correspond to asymptotic equilibria that are not homogeneous in the physical space. We then expect concentration solutions in the nonlinear case when

$$\frac{D_\psi^2}{V} < R\mu. \tag{70}$$

Notice that $D_\psi^2 = V^2$ when ψ is a Dirac delta and we recover, here in any dimension d, the linear stability region determined in the one-dimensional case in [36]. For any other choice of ψ, we have that $D_\psi^2 = V^2 + e$, where $e \geqslant 0$ is the variance of ψ. Then, when (59) is satisfied, the condition (69) with $D_\psi^2 = V^2 + e$ is automatically satisfied. In conclusion, the choice of ψ being a Dirac delta is the most unstable one, and, therefore, this choice makes computations feasible and allows to predict a wider instability region.

3.2. The Hamilton–Jacobi formalism and hydrodynamics

In this section, we investigate how the Hamilton–Jacobi formalism allows to characterise concentration solutions in the nonlinear case, in which the hydrodynamic equations do not allow to depict the concentration scenarios in all regimes. However, we expect that in a linearised regime the two approaches may give the same amount of information, like in the linear case (see section 2.4). As a consequence, we first consider the regime of small sensing radius R.

3.2.1. The regime R small. Let us now consider R small in the sense of (86) with $\mathcal{S} = \rho$, i.e.

$$0 < R \ll l_\rho := \frac{1}{\max \dfrac{|\nabla_x \rho|}{\rho}}. \tag{71}$$

Then, we may expand ρ as

$$\rho(t,x+R\hat{v}) \approx \rho(t,x) + R\hat{v}\cdot\nabla_x\rho(t,x),$$

so that the normalisation function of (58) is

$$c(t,x) \approx \rho(t,x)\,|\mathbb{S}^{d-1}|.$$

Therefore equation (57) becomes

$$\frac{\partial f}{\partial t}(t,x,v,\hat{v}) + \mathbf{v}\cdot\nabla_x f(t,x,v,\hat{v}) = \mu\left(\rho(t,x)\,\frac{1}{|\mathbb{S}^{d-1}|}\left[1 + R\hat{v}\cdot\frac{\nabla_x\rho(t,x)}{\rho(t,x)}\right] - f(t,x,v,\hat{v})\right). \tag{72}$$

The latter is a linearised kinetic equation in which $T[\rho]$ is evaluated in a small perturbation of a nondimensionalised homogeneous configuration $\rho^\infty = 1$, as $\dfrac{R\nabla_x\rho}{\rho}$ is small being $R \ll l_\rho$ (see the expression in the square brackets in (72)). This is exactly the regime in which the linear stability analysis is performed in [36]. When considering the rescaling (18) with the smallness regime (71), we have that

$$\mathbf{U}^\varepsilon_\rho = \varepsilon R V \frac{\nabla_x\rho}{\rho}, \qquad \mathbb{D}^\varepsilon_\rho = D^2_\psi\,\mathbb{I}.$$

Therefore the hydrodynamics (61), that is obtained by the rescaling (18), becomes

$$\partial_t\rho_\varepsilon = \varepsilon\nabla_x\cdot\nabla_x\cdot\left(\left(\frac{D^2_\psi}{\mu} - RV\right)\mathbb{I}\rho_\varepsilon\right) + \mathcal{O}\left(\varepsilon^2\right).$$

In the latter, the first order correction features a diffusion tensor whose positivity corresponds to the stability condition of the homogeneous configuration (69): specifically a positive diffusion corresponds to stability of the homogeneous configuration, while the negative diffusion corresponds to the emergence of patterns. The Hopf–Cole assumption in (72) with (18) leads to $G_R(p,v,\hat{v}) = \psi(v|\hat{v})(1 - R\hat{v}\cdot p)$.

3.2.2. An eikonal equation. Like in the linear case studied in section 2.4, we may also use the phase $\phi_\varepsilon = -\varepsilon\log\rho_\varepsilon$ in the aggregate equation (61). Letting $\varepsilon\to 0$ and assuming $\phi_\varepsilon\to\phi$, we formally obtain

$$\partial_t\phi + \mathbf{U}^G_R\cdot\nabla_x\phi + \nabla_x\phi^T\mathbb{D}^G_R\nabla_x\phi = 0, \tag{73}$$

because $\mathbf{U}^\varepsilon_\rho \to \mathbf{U}^G_R(\nabla_x\phi)$ (defined in (66) and $\mathbb{D}^\varepsilon_\rho \to \mathbb{D}^G_R(\nabla_x\phi)$, which is the variance covariance matrix of (62). Therefore, equation (73), in opposition to the linear case, is not the quadratic expansion near $\nabla_x\phi = 0$ of equation (64) except in the regime R small. In fact, in the linearised case (72) with (18), we have that

$$\partial_t\rho^0 + \nabla_x\cdot\left(\rho^0\mathbf{U}^0_\rho\right) = 0. \tag{74}$$

Moreover, as $G_R(p,v,\hat{v}) = \psi(v|\hat{v})(1-R\hat{v}\cdot p)$, then $\mathbf{U}^0_\rho = \mathbf{U}^G_R(0)$ and $\mathbb{D}^0_\rho = D^2_p H(0)$, so that like in the linear case, in this linearised regime obtained for R small, the eikonal equation (73) is a quadratic expansion of (64).

3.2.3. Dynamics of the concentration points. Concerning the concentration points dynamics, we remark that the hydrodynamics tell us that $x \in \Omega$ obeys

$$\dot{x}(t) = \mathbf{U}^0_\rho(x),$$

conversely, by repeating the same procedure as in section 2.4.2, we have that the Hamilton–Jacobi equation allows to conclude that a maximum point $\bar{x}_i$ satisfies

$$\dot{\bar{x}}_i(t) = \mathbf{U}^G_R(p).$$

The hydrodynamics and the WKB analysis give the same information concerning the dynamics of the maxima in the linearised case (71) as $\mathbf{U}^0_\rho = \mathbf{U}^G_R(0)$.

Conversely, for any R, the hydrodynamics do not allow to conclude anything in general about the maxima points, while the Hamilton–Jacobi equation allows to state that when $p = \nabla_x\varphi(\bar{x}_i) = 0$, then, as a consequence of (67)

$$\dot{\bar{x}}_i(t) = \int_{\mathbb{S}^{d-1}} V_\psi(\hat{v})\,\hat{v}\,\mathrm{d}\hat{v}.$$

The latter is a nonvanishing quantity in the case where $V_\psi(\hat{v})$ is not even as a function of $\hat{v}$. In such a case it is possible to observe moving patterns, as showed in [36].

Moreover, the Hamilton–Jacobi equation (64) also gives the microscopic concentration profile, that is not given by the hydrodynamics, not even in the linearised case. In the stability regime, i.e. when (59) is satisfied, we actually have that $p=0$ is a minimum of H as $H(0)=0$, $\nabla_p H(0)=0$ when V_ψ is even and $D^2_p H(0)$ is positive definite. Therefore, we have $H(p)>0\,\forall p\neq 0$ which implies that $\varphi(t,x)$ decreases and possible initial concentrations will disappear. In the instability regime (70), the situation is more interesting and the prototype of the shape of the Hamiltonian is depicted in figure 4. In fact, being $D^2_p H(0)$ negative definite, then $p=0$ is a maximum point of H. Therefore, there will be a range of values of p where the Hamiltonian is negative. As for $p\to\pm\infty$, $H\to\infty$, and if H is C^1, there will be a value $\bar{p}>0$ where $H(\pm\bar{p})$ is minimum (and negative). This explains the profile of the Hamiltonian obtained in figure 4. When $\nabla_x\varphi$ is small (which is the case near concentration points), then $H(\nabla_x\varphi)<0$, meaning that φ will increase and the concentration will get stronger. Then, the slopes $\pm\tilde{p}$ where $H(\pm\tilde{p})=0$ determine a saw tooth stationary state. This is independent of the initial condition, and in fact concentrations may arise also from initial homogeneous configurations (see figure 5).

3.3. An example

As an example, we consider the one dimensional eigenproblem (65) (when $d=1$ and $\hat{v}=\pm 1$). Then H is defined by

$$1 = \frac{\mu}{(\exp^{-Rp}+\exp^{Rp})}\int_0^U \psi(v|\hat{v})\left(\frac{\exp^{-Rp}}{\mu+H-vp}+\frac{\exp^{Rp}}{\mu+H+vp}\right)\mathrm{d}v,$$

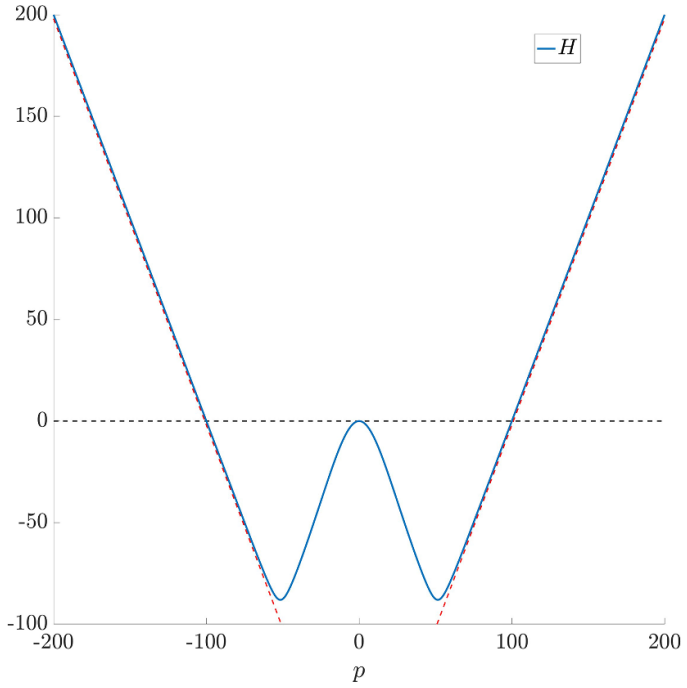

Figure 4. The convex-concave Hamiltonian H in the one-dimensional case as computed explicitly in formula (75). The values of μ, V, R are those corresponding to the example in section 3.3. The red dashed lines correspond to the asymptotes $\pm U|p|$, the black horizontal dashed line is the zero-level. The values $\pm\tilde{p} \neq 0$ with $H(\tilde{p}) = 0$ determine the slopes of the saw tooth solutions in figure 5.

which is also written

$$1 = \frac{\mu}{2\left(\exp^{-Rp} + \exp^{Rp}\right)} \int_0^U \psi\left(v|\hat{v}\right) \left(\frac{\exp^{-Rp}\left(\mu + H + vp\right) + \exp^{Rp}\left(\mu + H - vp\right)}{\left(\mu + H\right)^2 - v^2p^2} \right) \mathrm{d}v.$$

When $\psi(v|\hat{v}) = \delta(v - V)$, the latter reduces to

$$1 = \frac{\mu}{\exp^{-Rp} + \exp^{Rp}} \left(\frac{\exp^{-Rp}\left(\mu + H + Vp\right) + \exp^{Rp}\left(\mu + H - Vp\right)}{\left(\mu + H\right)^2 - V^2p^2} \right),$$

and, therefore

$$H^2 + H\mu - V^2p^2 + \mu V p D_R\left(p\right) = 0, \qquad D_R\left(p\right) = \frac{\exp^{Rp} - \exp^{-Rp}}{\exp^{-Rp} + \exp^{Rp}} = \tanh\left(Rp\right),$$

in such a way that

$$H\left(p\right) = \frac{-\mu + \sqrt{\mu^2 + 4V^2p^2 - 4\mu V p D_R\left(p\right)}}{2}. \tag{75}$$

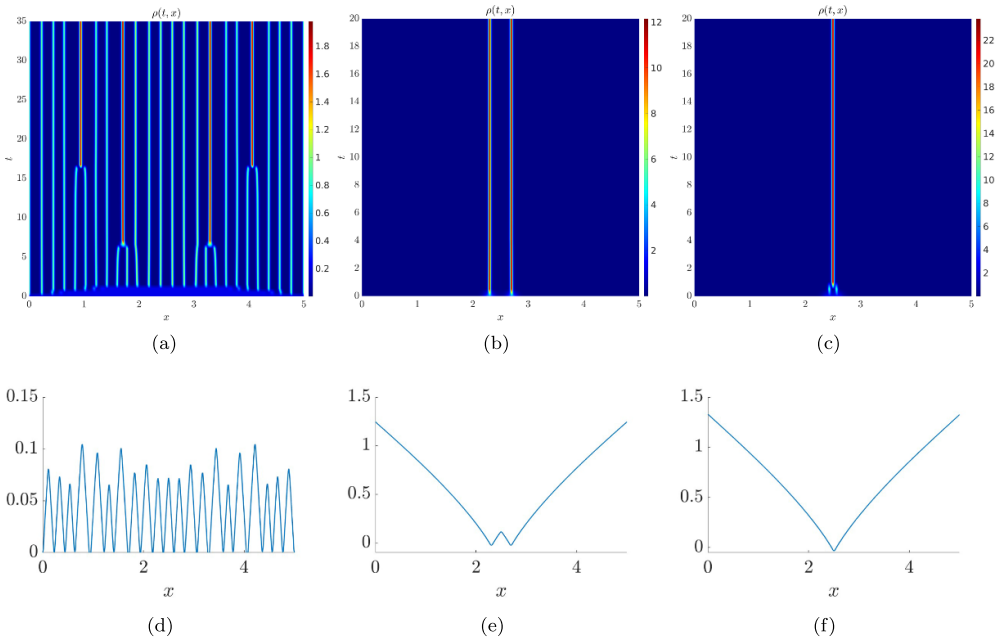

Figure 5. One dimensional example with parameters $V=1, \mu=100, R=5\cdot 10^{-2}$. In (a) the initial condition is the perturbation of the homogeneous configuration, in (b) the initial condition is a bimodal Gaussian centered in $\tilde{x}_1=2.3, \tilde{x}_2=2.7$, in (c) the initial condition is a bimodal Gaussian (i.e. ρ_0 as in (56)) centered in $\tilde{x}_1=2.4, \tilde{x}_2=2.6$. In the second line we report the corresponding profiles of $-\varepsilon\log(\rho(t,x))$, $\varepsilon=10^{-2}$. These saw tooth curves result from the convex-concave Hamiltonian in figure 4.

Consequently, the sign of H is determined by the sign of $V|p|-\mu|D_R(p)|$ and we obtain

$$H(p)>0 \qquad \text{iff} \qquad \frac{V}{\mu}>\frac{D_R(p)}{p}.$$

For $|p|$ small this is in accordance with the sign of the second derivative in formula (68). In the regime when $R|p|$ is small then $\dfrac{D_R(p)}{p}=\dfrac{\tanh(Rp)}{p}\sim R$ and the latter condition becomes (59). As $p=\nabla_x\varphi$ and $|\nabla_x\varphi|\approx\dfrac{|\nabla_x\rho|}{\rho}$, then it coherently corresponds to the analysis performed in the regime of R small. In general, the Hamiltonian (75) will have several (three if R is large enough) zeros, that are given by

$$p=0, \qquad \tilde{p}=D_R(\tilde{p}).$$

We now show some numerical tests. We solve numerically the kinetic equation (57) in the regime (18). In particular we choose the following parameter values: $V=1, \mu=100, R=5\cdot 10^{-2}$. Therefore $\varepsilon=10^{-2}$ and we are in the regime of linear instability as $\dfrac{V}{\mu R}=0.2$. We consider three different initial conditions: (a) a perturbation of the homogeneous configuration,

(b) a bimodal Gaussian (i.e. ρ^0 as in (56)) centered in $\tilde{x}_1 = 2.3, \tilde{x}_2 = 2.7$, (c) a bimodal Gaussian (i.e. ρ^0 as in (56)) with $\tilde{x}_1 = 2.4, \tilde{x}_2 = 2.6$.

As we are in a regime of linear instability, in figure 5(a) we observe pattern formation, while in figure (b), as the two initial peaks are far enough, they stay so along the dynamics. In figure 5(c) we have that the two peaks merge, because the sensing radius is large enough. In the second line (figures 5(d)–(f), respectively), we plot the corresponding $-\varepsilon \log(\rho_\varepsilon)$.

4. Conclusion

We have considered a kinetic equation with a BGK relaxation operator in which the transition probability is nonlocal in the physical space, and thus space-dependent. The transition kernel can be linear or nonlinear. For high frequencies, both in the localised (18) and nonlocalised (24) regime, we have explained the formation of concentration solutions by means of the real WKB ansatz, following [7], that leads in the limit to a Hamilton–Jacobi equation. This method, in the spirit of adaptive dynamics, provides us with the position evolution of the concentration points and with the concentration profiles. We have studied preliminarly the linear case, in order to be able to study the nonlinear one, in which the classical hydrodynamics does not allow to characterise completely the aggregation solutions. We can conclude that

- In the linear case at the leading order, the kinetic equation and corresponding aggregate limit (hydrodynamics) almost give a complete information that coincides with the one obtained by means of the WKB method through the Hamilton–Jacobi equation and the canonical equation for the concentration points toward the local maxima of the signal. As a plus, the WKB analysis allows also to determine the set of maximum points Ω_M and the correct concentration profile (4), (51) and (52). This leads to one of the main messages of the present paper that is to use the Hamilton–Jacobi formalism in order to study concentration solutions in more complex scenarios, such as the nonlinear one.
- In the nonlinear case, the same link holds between the aggregate limit analysis and the WKB analysis in the linearised regime (R small in the sense of (71)). When R is not small (and ρ is not smooth) and we expect concentrations, then stating (even formally) the hydrodynamic limit is not banal. Then, the WKB method gives more information with respect to the aggregate equation through the canonical equation for the maxima. A difference with respect to the linear case lies in the fact that it is not possible to find a condition for the location of the concentration points. However, the Hamilton–Jacobi formalism allows to determine the stability of the the homogeneous configuration or of concentration solutions. The latter case corresponds to an unusual convex-concave Hamiltonian, explaining saw tooth patterns which are obtained numerically. In particular, it is possible to recover the linear stability condition for the homogeneous configuration found in [36] in the special case of one dimension and ψ a Dirac delta in the limit of R small, where ψ being the Dirac delta was chosen in order to determine explicitly the instability condition. Furthermore, the present analysis actually shows that it is possible to extend the results of [36] to other distributions ψ that have a larger second moment with respect to the Dirac delta, that is the most unstable one, in the sense that it prescribes a larger parameters region where there is linear instability. Moreover, the Hamilton–Jacobi formalism allows to perform explicitly the analysis in any dimension and the study of the positivity of the Hessian matrix of the Hamiltonian allows to state the same stability result in any dimension.

Both in the linear and nonlinear cases the hydrodynamics and the WKB analysis give compatible eikonal equations in the suitable limit. While in the linear case concentrations have been characterised fully in both regimes (18)–(24), in the nonlinear case only the rescaling (18) could be considered and the location of the concentration points cannot be explicitly determined. Anyway, the WKB analysis, as a further contribution, allows to determine a concentration profile also in the fully nonlinear case (R not small), when the analysis of the aggregate limits is not banal and as it goes beyond the regime of the linear stability analysis. These considerations suggest that the WKB analysis could be used in order to extend the results of a linear stability analysis to other transition probabilities and in any dimension d. In fact, concerning the dimension d, the typical and complete dimension for studying, in general, cell migration, and specifically chemotaxis and cell-cell adhesion, *in-vivo*, is, of course, $d = 3$. However cell migration *in-vitro*, is typically studied with $d = 2$, and, also cell-cell adhesion, specifically when it leads to tissue formation. Nevertheless, the one-dimensional case $d = 1$ is interesting and has been considered extensively in order to study aggregation phenomena in presence of chemotaxis and cell sorting due to cell-cell adhesion when in presence of two different populations of cells, especially in nonlocal models (see e.g. [1]). Here we have presented numerical tests when $d = 1$ mainly for a matter of practicality on displaying the theoretical results.

In the context of the study of kinetic eikonal equations in the same spirit as [7], this work has allowed to make some steps further as (i) the Markovian probability in the relaxation operator depends on the spatial variable as it is nonlocal in the physical space, (ii) it was applied in order to study the space dependent equilibrium in a regime in which concentrations are shown, (iii) a regime in which the WKB and hydrodynamic limit procedure may commute was detected. Moreover, our condition (34) for the eigenproblem is new. Not only it generalises but it also simplifies that in [10].

Moreover, as T depends on x and on the small parameter ε, in the linear case H depends on both x and $\nabla_x \varphi$, then we obtain from (29) an evolution equation for H_ε, and, then, a time dependent eigenvalue problem similar to the principal bundle for parabolic equations. Another open problem is to determine the boundary conditions for the Hamilton–Jacobi equations.

Data availability statement

The data that support the findings of this study are available upon reasonable request from the authors.

Acknowledgment

N L is member of INdAM-GNFM. N L acknowledges support by the Italian Ministry for Education, University and Research (MUR) through the 'Dipartimenti di Eccellenza' Programme (2018- 2023) of the Department of Mathematical Sciences, G L Lagrange, Politecnico di Torino (CUP: E11G18000350001). N L gratefully acknowledges support from the Italian Ministry of University and Research (MUR) through the Grant PRIN2022-PNRR Project (No. P2022Z7ZAJ) 'A Unitary Mathematical Framework for Modelling Muscular Dystrophies' (CUP: E53D23018070001). N L gratefully acknowledges support from the CNRS International Research Project 'Modélisation de la biomécanique cellulaire et tissulaire' (MOCETIBI).

Appendix A. Aggregate behaviour (hydrodynamics)

A.1. Hyperbolic limit

In the regime defined by (17), we may find limiting equations for the averaged population quantities. The single conservation law induces that the aggregate quantity is the mass and we obtain an evolution equation for the number density ρ. Taking into account the equilibrium $T[\mathcal{S}]_\varepsilon$, the formal expansion of (17) at order $\mathcal{O}(\varepsilon)$ is a diffusion-advection equation with a dominating drift term and small diffusivity

$$\partial_t \rho_\varepsilon + \nabla_x \cdot (\rho_\varepsilon \mathbf{U}^\varepsilon_{\mathcal{S}}) = \varepsilon \nabla_x \cdot (\nabla_x \cdot \mathbb{D}^\varepsilon_{\mathcal{S}} \rho_\varepsilon + \rho_\varepsilon \mathbf{U}^\varepsilon_{\mathcal{S}} \nabla_x \cdot \mathbf{U}^\varepsilon_{\mathcal{S}}), \tag{76}$$

where $\mathbf{U}^\varepsilon_{\mathcal{S}}$ is the average of $T[\mathcal{S}]_\varepsilon$ and $\mathbb{D}^\varepsilon_{\mathcal{S}}$ its variance-covariance matrix as defined by (8) and (9). The first-order correction in (76) can be derived by determining the corrector f_1 in a Chapman-Enskog expansion of $f_\varepsilon = f_0 + \varepsilon f_1$; the appearance of the divergence of $\mathbf{U}^\varepsilon_{\mathcal{S}}$ is due to the fact that $T[\mathcal{S}]$, and thus $\mathbf{U}_{\mathcal{S}}$ is space-dependent [16, 24]. The boundary conditions can be found by imposing (15) to f_ε [40] and this gains

$$(\rho_\varepsilon \mathbf{U}^\varepsilon_{\mathcal{S}} - \varepsilon \big(\mathbb{D}^\varepsilon_{\mathcal{S}} \nabla_x \rho_\varepsilon + \rho_\varepsilon (\nabla_x \cdot \mathbb{D}^\varepsilon_{\mathcal{S}} + \mathbf{U}^\varepsilon_{\mathcal{S}} \nabla_x \cdot \mathbf{U}^\varepsilon_{\mathcal{S}})\big) \cdot \boldsymbol{n} = 0 \qquad \text{on } \partial\Omega. \tag{77}$$

In the asymptotic limit $\varepsilon \to 0^+$, the dynamics is ruled by the equilibrium of (17) at order zero in ε, that is defined by

$$f_0 = \rho T[\mathcal{S}]_0, \qquad T[\mathcal{S}]_0 := \lim_{\varepsilon \to 0^+} T[\mathcal{S}]_\varepsilon,$$

in such a way that the evolution equation for $\rho = \rho_0$ is

$$\partial_t \rho + \nabla_x \cdot \left(\rho \mathbf{U}^0_{\mathcal{S}}\right) = 0. \tag{78}$$

For this conservation law, the no-flux boundary conditions that can be derived from (15) are given by

$$\rho \mathbf{U}^0_{\mathcal{S}}(x) \cdot \boldsymbol{n}(x) = 0, \quad \text{for } x \in \partial\Omega, \tag{79}$$

As explained in appendix B, the latter are actually only to be imposed on the entering region, but this can be in fact derived by the underlying kinetic boundary conditions that are imposed on the entering zone $\Gamma_-(x)$.

In conclusion, both rescalings, the local macroscopic one (18) or the nonlocal microscopic one (24), are possible and lead to the same equation (78), but the scales of the sensing radius differ and, as a consequence, $\mathbf{U}^0_{\mathcal{S}}$ differs. For example, in the case $b(\mathcal{S}) = \mathcal{S}$, when the rescaling (18) is performed (assuming $\mathcal{S}$ smooth), then $T[\mathcal{S}]_\varepsilon(v, \hat{v}) = c(x)\psi(v|\hat{v})\mathcal{S}(x + \varepsilon R\hat{v})$, so that

$$T[\mathcal{S}]_0(v, \hat{v}) = \psi(v|\hat{v}) \frac{1}{|\mathbb{S}^{d-1}|}, \quad \mathbf{U}^0_{\mathcal{S}} = \int_{\mathbb{S}^{d-1}} V_\psi(\hat{v})\, \hat{v} \mathrm{d}\hat{v}, \quad \mathbb{D}^0_{\mathcal{S}} = D^2_\psi \mathbb{I},$$

where $V_\psi(\hat{v}), D^2_\psi$ are defined in (6). If $V_\psi(\hat{v})$ is even (e.g. V_ψ constant), then $\mathbf{U}^0_{\mathcal{S}} = 0$, so that from (76) $\partial_t \rho_0 = 0$. Anyway, localisation does not imply a vanishing drift in all cases. Let us, for example, assume a comparative sensing [34], which means that the turning rate depends on what is measured in $x + R\hat{v}$ and $x - R\hat{v}$, i.e.

$$b(\mathcal{S}(x + \lambda\hat{v}), \mathcal{S}(x - \lambda\hat{v})) = \alpha + \beta \frac{\mathcal{S}(x - \lambda\hat{v}) - \mathcal{S}(x + \lambda\hat{v})}{2k + \mathcal{S}(x + \lambda\hat{v}) + \mathcal{S}(x - \lambda\hat{v})}.$$

Then, in the fast adaptation regime $\beta \to \frac{\beta}{\varepsilon}$, we find

$$T[\mathcal{S}]_0(v,\hat{v}) = \frac{\psi(v|\hat{v})}{\alpha|\mathbb{S}^{d-1}|}\left(\alpha + \beta\frac{R\nabla_x \mathcal{S}(x)\cdot\hat{v}}{k+\mathcal{S}(x)}\right),$$

which means that, even in the localised interactions regime, if $T[\mathcal{S}]$ is given by a comparative sensing, the equilibrium depends on the directional derivative of the external field $\mathcal{S}$ along each microscopic direction $\hat{v}$. Conversely, in the regime (24) we have,

$$T[\mathcal{S}]_0 = T[\mathcal{S}], \quad \text{and thus,} \quad \mathbf{U}^0_{\mathcal{S}} = c(x)\int_{\mathbb{S}^{d-1}} V_\psi(\hat{v})\,\mathcal{S}(x+R\hat{v})\,\hat{v}\mathrm{d}\hat{v},$$

that is in general a nonvanishing quantity at the microscopic space scale. In fact, we can remark that even in the case $V_\psi(\hat{v}) = V_\psi$, then

$$\mathbf{U}^0_{\mathcal{S}} = V_\psi\, c(x)\int_{\mathbb{S}^{d-1}} \mathcal{S}(x+R\hat{v})\,\hat{v}\mathrm{d}\hat{v}$$

is a nonvanishing quantity unless $\mathcal{S}$ is spatially homogeneous. Therefore, the dominating drift term is due to the spatial heterogeneity that is sensed nonlocally.

In conclusion, equation (78), if derived as a large scale limit in the regime (18), has to be meant as a hydrodynamic limit on a macroscopic space scale in which interactions are localised and the (now local) equilibrium is reached fast as a longtime scale is observed. Conversely, regime (24) implies a high frequency and small speeds regime on the microscopic space scale and slow time scale that is the same as the one of the original kinetic equation (1). Therefore, when derived in this regime, equation (78) describes the evolution of the average number density on the original (microscopic) phase space.

A.2. Diffusive limit

When dealing with cell migration modeling, the diffusive rescaling is usual. In the present framework, it corresponds to choosing in the nondimensionalisation a diffusive long time scale $t_0 = \dfrac{L^2}{V^2}$ that actually satisfies $t_0 = \dfrac{\varepsilon^{-2}}{\mu}$, in such a way that $\mathrm{St} = \varepsilon$. Therefore, the rescaled kinetic equation is in the form

$$\partial_t f_\varepsilon + \frac{1}{\varepsilon}\mathbf{v}\cdot\nabla_x f_\varepsilon = \frac{1}{\varepsilon^2}\left(\rho_\varepsilon T[\mathcal{S}]_\varepsilon - f_\varepsilon\right). \tag{80}$$

When we consider a nonlocal diffusive rescaling, i.e.

$$(t,v,x) \to \left(\frac{t}{\varepsilon^2}, \varepsilon v, x\right) \tag{81}$$

and $T[\mathcal{S}]$ depends on x and on $(v,\hat{v})$, then typically $\mathbf{U}_{\mathcal{S}}$ is not a vanishing quantity and the aggregate equation for ρ is

$$\partial_t\rho + \nabla_x\cdot(\mathbf{U}_{\mathcal{S}}\rho) = \nabla_x\cdot\nabla_x\cdot(\rho\mathbb{D}_{\mathcal{S}}). \tag{82}$$

Conversely, when we consider a localised diffusive scaling, i.e.

$$(t,v,x) \to \left(\frac{t}{\varepsilon^2}, v, \frac{x}{\varepsilon}\right) \tag{83}$$

we can typically consider a Hilbert expansion for f_ε and $T[\mathcal{S}]_\varepsilon$, i.e.

$$f_\varepsilon = f_0 + \varepsilon f_1 + \mathcal{O}\left(\varepsilon^2\right) \qquad \int_{\mathcal{V}} f_0 \mathrm{d}v\mathrm{d}\hat{v} = \rho, \quad \int_{\mathcal{V}} f_1 \mathrm{d}v\mathrm{d}\hat{v} = 0,$$

and

$$T[\mathcal{S}]_\varepsilon = T[\mathcal{S}]_0 + \varepsilon T[\mathcal{S}]_1 + \mathcal{O}\left(\varepsilon^2\right), \qquad \int_{\mathcal{V}} T[\mathcal{S}]_0 \,\mathrm{d}v\mathrm{d}\hat{v} = 1, \quad \int_{\mathcal{V}} T[\mathcal{S}]_1 \,\mathrm{d}v\mathrm{d}\hat{v} = 0.$$

Comparing equal orders of ε we get $p_0 = \rho T[\mathcal{S}]_0$ at the leading order, at the first order the solvability condition $\mathbf{U}^0_{\mathcal{S}} = 0$ allows to determine the first order correction p_1 and integrating the second order, one gets the macroscopic equation for $\rho = \rho_0$

$$\partial_t \rho + \nabla_x \cdot \left(\mathbf{U}^1_{\mathcal{S}} \rho\right) = \nabla_x \cdot \nabla_x \cdot \left(\rho \mathbb{D}^0_{\mathcal{S}}\right), \tag{84}$$

where $\mathbf{U}^1_{\mathcal{S}}$ is the first moment of $T[\mathcal{S}]_1$ and $\mathbb{D}^0_{\mathcal{S}}$ is the variance-covariance matrix of $T[\mathcal{S}]_0$ (see [34] for details). Then, supposing that

$$\mathbb{D}^0_{\mathcal{S}} = \nu^2 \bar{\mathbb{D}}^0_{\mathcal{S}}, \tag{85}$$

when $\nu^2 = \varepsilon$, i.e. for a small diffusivity, we essentially recover (76) in the macroscopic limit.

A.3. Limit for small R

Let us define the characteristic length of variation of $\mathcal{S}$ and its ratio to the sensing radius as

$$l_{\mathcal{S}} := \frac{1}{\max \dfrac{|\nabla_x \mathcal{S}|}{\mathcal{S}}}, \qquad \eta_{\mathcal{S}} := \frac{R}{l_{\mathcal{S}}}. \tag{86}$$

We remark that when $R \ll l_{\mathcal{S}}$, then we may consider the Taylor expansion of $\mathcal{S}$ at first order

$$\mathcal{S}\left(x + R\hat{v}\right) = \mathcal{S}\left(x\right) + R\hat{v} \cdot \nabla_x \mathcal{S}\left(x\right) + \mathcal{O}\left(R^2\right),$$

that is a positive quantity. Then, for example, in the case $b(\mathcal{S}) = \mathcal{S}$, we may approximate the probability density function $T[\mathcal{S}]$ as

$$\begin{aligned} T[\mathcal{S}]\left(v,\hat{v}\right) &= T[\mathcal{S}]_0\left(v,\hat{v}\right) + T[\mathcal{S}]_1\left(v,\hat{v}\right), \\ T[\mathcal{S}]_0\left(v,\hat{v}\right) &= \frac{\psi\left(v|\hat{v}\right)}{|\mathbb{S}^{d-1}|}, \quad T[\mathcal{S}]_1\left(v,\hat{v}\right) = \frac{\psi\left(v|\hat{v}\right)}{|\mathbb{S}^{d-1}|} R\hat{v} \cdot \frac{\nabla_x \mathcal{S}\left(x\right)}{\mathcal{S}\left(x\right)}. \end{aligned}$$

Then, choosing $L = l_{\mathcal{S}}$ the nondimensionalisation of (1) leads to

$$\mathrm{St}\,\partial_t f_\varepsilon\left(t,x,v,\hat{v}\right) + \mathbf{v} \cdot \nabla_x f_\varepsilon\left(t,x,v,\hat{v}\right) = \frac{1}{\mathrm{Kn}}\left(\rho_\varepsilon\left(t,x\right) \frac{\psi\left(v|\hat{v}\right)}{|\mathbb{S}^{d-1}|}\left(1 + \eta_{\mathcal{S}} \hat{v} \cdot \frac{\nabla_x \mathcal{S}\left(x\right)}{\mathcal{S}\left(x\right)}\right) - f_\varepsilon\left(t,x,v,\hat{v}\right)\right).$$

With the choice $\dfrac{1}{L} \sim \varepsilon$, that amounts to (18), then we obtain $\eta_{\mathcal{S}} = R\varepsilon$ and equation (1) becomes

$$\partial_t f_\varepsilon\left(t,x,v,\hat{v}\right) + \mathbf{v} \cdot \nabla_x f_\varepsilon\left(t,x,v,\hat{v}\right) = \frac{1}{\varepsilon}\left(\rho_\varepsilon\left(t,x\right)\left(T[\mathcal{S}]_0 + \varepsilon T[\mathcal{S}]_1\right) - f_\varepsilon\left(t,x,v,\hat{v}\right)\right).$$

The leading order term is local while the role of the sensing radius enters the dynamics as a higher order term. In this case the evolution equations for ρ_ε correspond in the macroscopic point of view (18) and in the high frequency (microscopic) one (24), i.e.

$$\partial_t \rho_\varepsilon = \varepsilon \Delta \rho_\varepsilon. \tag{87}$$

When choosing the diffusive scaling (choosing V_ψ constant for simplicity) we obtain (84) with $\mathbb{D}^0_{\mathcal{S}} = \mathbb{I}$ and $\mathbf{U}^1_{\mathcal{S}} = R\dfrac{\nabla_x \mathcal{S}}{\mathcal{S}}$, that is the Keller-Segel model [27, 34].

Appendix B. Boundary conditions

In section 1.2 we have shown the boundary conditions for the hyperbolic limit (78) of the kinetic equation (1) that are given by (79). In particular, both (78) and (79) are derived from the kinetic equation: (78) is derived from (17) and (79) are derived from (15) that is satisfied by any f that obeys kinetic boundary conditions in the form (13). The kinetic boundary conditions (13) are actually imposed on the entering boundary, i.e. on $\Gamma_-(x)$. The derived aggregate boundary conditions are noflux boundary conditions for the conservation law (78). Actually, we want to verify that those boundary conditions are to be imposed on the entering zone only, i.e. for $x \in \partial\Omega$ such that $\mathbf{U}^0_{\mathcal{S}}(x) \cdot \boldsymbol{n}(x) < 0$ as in the outgoing region, i.e. for $x \in \partial\Omega$ such that $\mathbf{U}^0_{\mathcal{S}} \cdot \boldsymbol{n} > 0$ they are granted by the underlying kinetic boundary conditions.

Therefore, we need to compute the average $\mathbf{U}^0_{\mathcal{S}}(x)$ for $x \in \partial\Omega$ that we denote as $\mathbf{U}^0_{\mathcal{S}_{|\partial\Omega}}$. First of all we need to define $T[\mathcal{S}]_{0_{|\partial\Omega}}$. Working in the regime (24), we define it as

$$T[\mathcal{S}]_{0_{|\partial\Omega}}(v,\hat{v}) = c(x)\, b\left(\mathcal{S}\left(x + R(x,\hat{v})\,\hat{v}\right)\right) \psi_{|\partial\Omega}(v|\hat{v}),$$

where $R(x,\hat{v})$ is defined in (10) and $\psi_{|\partial\Omega}(v|\hat{v})$ is to be dependent on $x \in \partial\Omega$, as for $\hat{v}\cdot\boldsymbol{n}(x) > 0$, then we should set $V_\psi = 0$. Therefore, we have that

$$T[\mathcal{S}]_{0_{|\partial\Omega}}(v,\hat{v}) = \begin{cases} \dfrac{\psi_{|\partial\Omega}(v|\hat{v})}{|\mathbb{S}^{d-1}|} & \text{if} \quad \hat{v}\cdot\boldsymbol{n} > 0, \\ c(x)\, b\left(\mathcal{S}\left(x + R\hat{v}\right)\right) \psi_{|\partial\Omega}(v|\hat{v}) & \text{if} \quad \hat{v}\cdot\boldsymbol{n} < 0, \end{cases}$$

as when $\hat{v}\cdot\boldsymbol{n}(x) > 0$ then $R(x,\hat{v}) = 0$, while when $\hat{v}\cdot\boldsymbol{n} < 0$, $x + R\hat{v} \in \Omega$ if, for example Ω is convex.

Now, as $T[\mathcal{S}]_0$ is in fact the equilibrium, it must satisfy the boundary conditions (13). We analyse the two cases $\alpha = 0$ (purely Maxwellian) and $\alpha = 1$ (pure reflection), any case in between follows as a convex combination. If we consider the Maxwellian boundary conditions, then we have

$$M(x,v,\hat{v}) = c(x) b(\mathcal{S}(x + R(x,\hat{v})\hat{v}) \psi_{|\partial\Omega}(v|\hat{v}), \qquad \hat{v} \in \Gamma_-(x),$$

and

$$\begin{aligned} \mathbf{U}^0_{\mathcal{S}_{\partial\Omega}} &= \left[\int_0^U v \left(\int_{\hat{v}\cdot\boldsymbol{n}<0} M(x,v,\hat{v})\,\hat{v}\mathrm{d}\hat{v} + \int_{\hat{v}\cdot\boldsymbol{n}>0} \frac{1}{|\mathbb{S}^{d-1}|}\psi(v|\hat{v})\,\hat{v}\mathrm{d}\hat{v}\right)\mathrm{d}v\right] \\ &= \int_0^U v \int_{\hat{v}\cdot\boldsymbol{n}<0} M(x,v,\hat{v})\,\hat{v}\mathrm{d}\hat{v}\mathrm{d}v. \end{aligned}$$

Therefore

$$\mathbf{U}^0_{\mathcal{S}_{\partial\Omega}} \cdot \boldsymbol{n} = \int_0^U v \int_{\hat{v}\cdot\boldsymbol{n}<0} M(x,v,\hat{v})\,\hat{v}\cdot\boldsymbol{n}\mathrm{d}\hat{v}\mathrm{d}v < 0.$$

In conclusion the whole boundary is an entering zone and then we need to impose (77). If $\alpha = 1$, then $T[\mathcal{S}]_0$ must satisfy the following boundary conditions, if $\hat{v} \in \Gamma_-(x)$

$$T[\mathcal{S}](v,\hat{v})_{\Gamma_-} = T[\mathcal{S}](v,\mathcal{W}(\hat{v})),$$

and here $\mathcal{W}(\hat{v})\cdot\boldsymbol{n} > 0$. Therefore $T[\mathcal{S}]_{|\Gamma_-} = \dfrac{\psi_{|\partial\Omega}(v|\hat{v})}{|\mathbb{S}^{d-1}|}$. In conclusion, following the same computations as for the case $\alpha = 0$, we find $\mathbf{U}^0_{\mathcal{S}} = 0$, i.e. the velocity vector vanishes on the whole boundary and (77) is satisfied.

Conversely, in the regime (18), we have that if $T[\mathcal{S}]_0$ does not depend on $\hat{v}$ (and on x) because of the localisation, then $\mathbf{U}^0_{\mathcal{S}} = 0$ on $\partial\Omega$.

ORCID iDs

Nadia Loy https://orcid.org/0000-0002-0705-8489
Benoît Perthame https://orcid.org/0000-0002-7091-1200

References

[1] Armstrong N J, Painter K J and Sherratt J A 2006 A continuum approach to modelling cell-cell adhesion *J. Theor. Biol.* **243** 98–113
[2] Barles G 1994 *Solutions de Viscosité des équations de Hamilton-Jacobi* (Springer)
[3] Barles G, Evans L C and Souganidis P E 1990 Wavefront propagation for reaction diffusion systems of pde *Duke Math. J.* **61** 835–58
[4] Barles G and Perthame B 2007 Concentrations and constrained Hamilton-Jacobi equations arising in adpative dynamics *Contemporary Mathematics* vol 439 p 57
[5] Bouin E 2015 A hamilton-jacobi approach for front propagation in kinetic equations *Kinet. Relat. Mod.* **8** 255–80
[6] Bouin E and Caillerie N 2019 Spreading in kinetic reaction-transport equations in higher velocity dimensions *Eur. J. Appl. Math.* **30** 219–47
[7] Bouin E and Calvez V 2012 A kinetic eikonal equation *C. R. Math.* **350** 243–8
[8] Bouin E, Calvez V, Grenier E and Nadin G 2023 Large-scale asymptotics of velocity-jump processes and nonlocal Hamilton-Jacobi equations *J. London Math. Soc.* **108** 141–89
[9] Bouin E, Calvez V and Nadin G 2015 Propagation in a kinetic reaction-transport equation: travelling waves and accelerating fronts *Arch. Ration. Mech. Anal.* **217** 08
[10] Caillerie N 2021 Large deviations of a forced velocity-jump process with a Hamilton–Jacobi approach *Ann. Inst. Fourier* **71** 1733–55
[11] Calvez V, Raoul G and Schmeiser C 2015 Confinement by biased velocity jumps: aggregation of escherichia coli *Kinet. Relat. Mod.* **8** 651–66
[12] Cercignani C 1987 *The Boltzmann equation and its Applications* (Springer)
[13] Chalub F A C C, Markowich P A, Perthame B and Schmeiser C 2004 Kinetic models for chemotaxis and their drift-diffusion limits *Monatshefte Math.* **142** 123–41
[14] Chauviere A, Hillen T and Preziosi L 2007 Modeling cell movement in anisotropic and heterogeneous network tissues *Netw. Heterog. Media* **2** 333
[15] Chen L, Painter K, Surulescu C and Zhigun A 2020 Mathematical models for cell migration: a non-local perspective *Phil. Trans. R. Soc.* B **375** 20190379
[16] Conte M and Loy N 2024 A non-local kinetic model for cell migration: a study of the interplay between contact guidance and steric hindrance *SIAM J. Appl. Math.* **84** S429–51

[17] Conte M and Loy N 2022 Multi-cue kinetic model with non-local sensing for cell migration on a fiber network with chemotaxis *Bull. Math. Biol.* **84** 42
[18] Crandall M G, Ishii H and Lions P-L 1992 User's guide to viscosity solutions of second order partial differential equations *Bull. Am. Math. Soc* **27** 1–67
[19] Diekmann O, Jabin P-E, Mischler S and Perthame B 2005 The dynamics of adaptation: an illuminating example and a Hamilton-Jacobi approach *Theor. Population Biol.* **67** 257–71
[20] Evans L 1989 The perturbed test function method for viscosity solutions of nonlinear PDE *Proc. R. Soc.* A **111** 359–75
[21] Filbet F, Laurencot P and Perthame B 2005 Derivation of hyperbolic models for chemosensitive movement *J. Math. Biol.* **50** 189–207
[22] Filbet F and Vauchelet N 2010 Numerical simulation of a kinetic model for chemotaxis *Kinet. Relat. Mod.* **3** B348–66
[23] Fleming W H and Souganidis P E 1986 Pde-viscosity solution approach to some problems of large deviations *Ann. Scuola Nor. Super. Pisa-Class. Sci.* **13** 171–92
[24] Hillen T 2006 M5 mesoscopic and macroscopic models for mesenchymal motion *J. Math. Biol.* **53** 585–616
[25] Hillen T and Othmer H G 2000 The diffusion limit of transport equations derived from velocity-jump processes *SIAM J. Appl. Math.* **61** 751–75
[26] Hillen T, Painter K and Schmeiser C 2007 Global existence for chemotaxis with finite sampling radius *Discrete Contin. Dyn. Syst.* B **7** 125–44
[27] Keller E F and Segel L A 1970 Initiation of slime mold aggregation viewed as an instability *J. Theor. Biol.* **26** 399–415
[28] Lam K and Lou Y 2022 *Introduction to Reaction-Diffusion Equations* (*Lecture Notes on Mathematical Modelling in the Life Sciences*) (Springer)
[29] Lam K, Lou Y and Perthame B 2023 A Hamilton-Jacobi approach to evolution of dispersal *Commun. PDE* **48** 86–118
[30] Lods B 2005 Semigroup generation properties of streaming operators with noncontractive boundary conditions *Math. Comput. Modelling* **42** 1441–62
[31] Lorenzi T and Pouchol C 2020 Asymptotic analysis of selection-mutation models in the presence of multiple fitness peaks *Nonlinearity* **33** 5791
[32] Lorz A, Mirrahimi S and Perthame B 2011 Dirac mass dynamics in multidimensional nonlocal parabolic equations *Commun. PDE* **36** 1071–98
[33] Loy N, Hillen T and Painter K 2022 Direction dependent turning leads to anisotropic diffusion and persistence *Eur. J. Appl. Math.* **33** 729–65
[34] Loy N and Preziosi L 2020 Kinetic models with non-local sensing determining cell polarization and speed according to independent cues *J. Math. Biol.* **80** 373–421
[35] Loy N and Preziosi L 2020 Modelling physical limits of migration by a kinetic model with non-local sensing *J. Math. Biol.* **80** 1759–801
[36] Loy N and Preziosi L 2020 Stability of a non-local kinetic model for cell migration with density dependent orientation bias *Kinet. Relat. Mod.* **13** 1007–27
[37] Loy N and Preziosi L 2021 Stability of a non–local kinetic model for cell migration with density–dependent speed *Math. Med. Biol.* **38** 83–105
[38] Othmer H and Hillen T 2002 The diffusion limit of transport equations ii: Chemotaxis equations *SIAM J. Appl. Math.* **62** 1222–50
[39] Othmer H G, Dunbar S R and Alt W 1988 Models of dispersal in biological systems *J. Math. Biol.* **26** 263–98
[40] Plaza R G 2019 Derivation of a bacterial nutrient-taxis system with doubly degenerate cross-diffusion as the parabolic limit of a velocity-jump process *J. Math. Biol.* **78** 1681–711
[41] Stroock D W 1974 Some stochastic processes which arise from a model of the motion of a bacterium *Z. Wahrscheinlichkeitstheor. Verwandte Geb.* **28** 305–15